iScience

CellPress
OPEN ACCESS

Article

Mulberroside A alleviates osteoarthritis via restoring impaired autophagy and suppressing MAPK/NF-κB/PI3K-AKT-mTOR signaling pathways

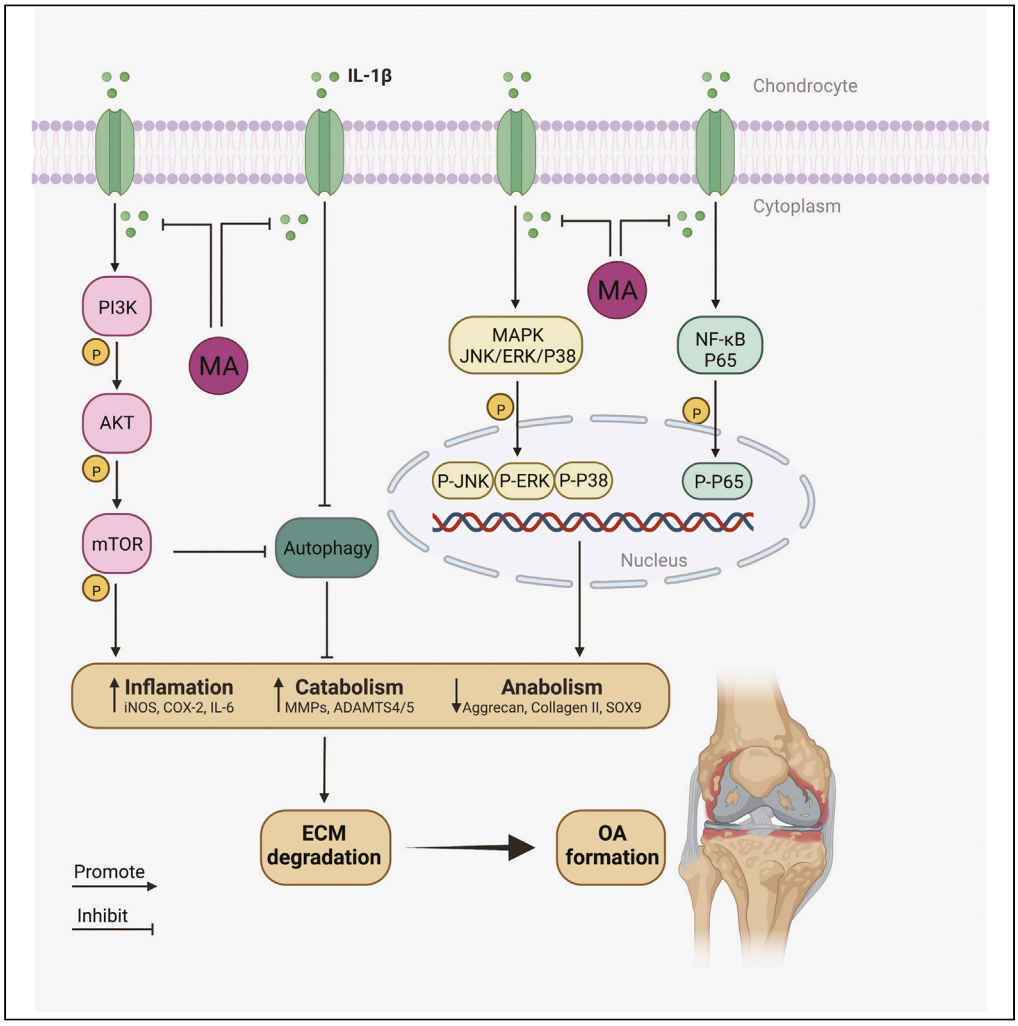

Rui Lu, Zhenni Wei, Zhenggang Wang, ..., Fengjing Guo, Shuang Liang, Anmin Chen

liangshuang0310@tjh.tjmu.edu.cn (S.L.)
anminchen@hust.edu.cn (A.-m.C.)

Highlights

Osteoarthritis (OA) is a disease mechanized by inflammation and impaired autophagy

Mulberroside A (MA), a natural product, has biological activities in various diseases

MA alleviates OA by inhibiting inflammation and enhancing autophagy signaling pathways

Lu et al., iScience 26, 105936
February 17, 2023
https://doi.org/10.1016/j.isci.2023.105936

iScience

CellPress
OPEN ACCESS

Article

Mulberroside A alleviates osteoarthritis via restoring impaired autophagy and suppressing MAPK/NF-κB/PI3K-AKT-mTOR signaling pathways

Rui Lu,[1] Zhenni Wei,[2] Zhenggang Wang,[1,3] Shimeng Xu,[1] Kai Sun,[1] Peng Cheng,[1] Xiaojian Huang,[1] Hongbo You,[1] Fengjing Guo,[1] Shuang Liang,[1,4,5,*] and An-min Chen[1,4,*]

SUMMARY

Osteoarthritis (OA) is a trauma-/age-related degenerative disease characterized by chronic inflammation as one of its pathogenic mechanisms. Mulberroside A (MA), a natural bioactive withanolide, demonstrates anti-inflammatory properties in various diseases; however, little is known about the effect of MA on OA. We aim to examine the role of MA on OA and to identify the potential mechanisms through which it protects articular cartilage. *In vitro*, MA improved inflammatory response, anabolism, and catabolism in IL-1β-induced OA chondrocytes. The chondroprotective effects of MA were attributed to suppressing the MAPK, NF-κB, and PI3K-AKT-mTOR signaling pathways, as well as promoting the autophagy process. *In vivo*, intra-articular injection of MA reduced the cartilage destruction and reversed the change of anabolic and catabolic-related proteins in destabilized medial meniscus (DMM)-induced OA models. Thus, the study indicates that MA exhibits a chondroprotective effect and might be a promising agent for OA treatment.

INTRODUCTION

Osteoarthritis (OA) is a common degenerative joint disease that occurs mainly in patients with prior joint trauma and the elderly and is characterized by pain, swelling, limited mobility, and deformity.[1] The high-risk groups of OA include joint trauma, individuals with the age over 65, and obesity.[2] Treatment for OA includes conservative treatment and surgical treatment. Mild patients are recommended to reduce joint activities and give anti-inflammatory and analgesic treatment; for end-stage patients, joint replacement surgery is recommended to relieve joint pain and restore certain functions.[3] Due to the high incidence, long treatment cycle, and side effects such as gastrointestinal inflammation and liver damage from drug therapy, OA has caused a great economic burden to the society.[4] Therefore, finding suitable drugs or exploring the pathogenesis of OA is a way of solving the problem.

Cartilage is the most critical component of the joint and directly affects the development and progression of OA.[5] Chondrocytes, the only cell type within cartilage, and the extracellular matrix (ECM) are important components for maintaining cartilage function.[6] Increased catabolism and decreased anabolism in chondrocytes can trigger the degradation of ECM.[7] The pathogenesis of OA is still unclear, but it is mainly believed to be related to chronic inflammation.[8] Enhanced inflammatory responses lead to increased catabolism and decreased anabolism in chondrocytes, which in turn trigger the degradation of the ECM. The enhancement of inflammatory response is closely related to the activation of MAPK (mitogen-activated protein kinase) and NF-κB (nuclear factor kappa-light-chain-enhancer of activated B cells) signaling pathways, and studies have demonstrated that MAPK and NF-κB signaling pathways play an important role in promoting the progression of OA.[9] Furthermore, autophagy process, an intracellular protective mechanism, is regulated by the PI3K-AKT-mTOR signaling pathway and is also considered to be a crucial factor in maintaining the stability of cartilage, as impaired autophagy will contribute to the apoptosis of chondrocytes and the degradation of the ECM.[10]

Mulberroside A (MA) is a natural bioactive component isolated from Mori Cortex which has anti-inflammatory, antitussive, and diuretic characteristics and is widely used in Korea.[11] Studies have shown that MA has the anti-inflammatory and analgesic activities,[12] possesses the properties of anti-hyperuricemia,[13,14] inhibition of melanin formation[15] and NF-κB signaling pathway.[11,16] However, little information is available about the effect

[1]Department of Orthopedics, Tongji Hospital, Tongji Medical College, Huazhong University of Science and Technology, Wuhan 430030, China

[2]Wuhan Institute of Biological Products, Co. Ltd, Wuhan 430207, China

[3]Department of Physiology and Pharmacology, Karolinska Institutet, 17177 Stockholm, Sweden

[4]These authors contributed equally

[5]Lead contact

*Correspondence: liangshuang0310@tjh.tjmu.edu.cn (S.L.), anminchen@hust.edu.cn (A.-m.C.)

https://doi.org/10.1016/j.isci.2023.105936

of MA on OA. In recent years, studies have shown the potential role of plant-derived anti-inflammatory components such as artesunate[17] and physalin a[18] in slowing cartilage degradation, suggesting the existence of alternative strategies for OA treatment. Considering the pathogenic role of inflammatory response in OA and the anti-inflammatory properties of MA, we designed this experiment to explore the role of MA in OA.

RESULTS

Identification of mice articular chondrocytes *in vitro*

Articular cartilage is composed of chondrocytes and cartilage matrix. Chondrocytes are the only cellular components of articular cartilage.[19] Changes in their biological properties are closely related to the occurrence and development of OA.[20] Cells extracted from mice articular cartilage were identified by observing cells morphology, toluidine blue staining, safranin o staining, and collagen II immunofluorescence staining. In our experiments, we observed that the primary cells were polygonal or triangular, and the cells of the first passage generation were mostly oval, with round or oval nuclei and abundant cytoplasm (Figure 1A). Toluidine blue staining of normal primary chondrocytes showed that there were blue-purple metachromatic granules in the cells, and a small amount of metachromatic granules appeared around the cells (Figure 1B). Besides, chondrocytes are rich in proteoglycans, which can be reflected by safranin o staining (Figure 1C). In addition, chondrocytes have no specific markers that can be detected, but can produce large amounts of collagen II,[21] which are the main components of the cartilage matrix and can be detected in the cytoplasm using immunofluorescence methods (Figure 1D). Combined with the parts taken of the cells and the observed features mentioned above, it is confirmed that the cells observed in this experiment are chondrocytes.

Viability of chondrocytes treated with IL-1β/MA and selection of an optimal concentration of Mulberroside A

The effect of IL-1β and MA on the viability of chondrocytes was evaluated by a CCK8 assay. As shown in Figure 1F, CCK-8 assay found that MA at the concentration of 80 μM affected the viability of chondrocytes ($p < 0.05$), while MA at or below 40 μM did not affect the cell viability ($p > 0.05$). Besides, the viability of chondrocytes was not significantly affected when chondrocytes were stimulated with 5 ng/mL IL-1β or 40 μM MA alone or together for 24 h ($p > 0.05$). Afterward, western blot analysis was applied to the selection of an optimal concentration of MA on chondrocytes. Cells were treated with 5 ng/mL IL-1β alone or accompanied with different concentrations of MA (5, 10, 20, and 40 μM) for 24 h. Data revealed that MA at the concentrations of 20 μM or 40 μM promoted anabolism, inhibited catabolism and inflammatory metabolism in IL-1β-induced chondrocytes, of which MA at a concentration of 40 μM has a more obvious effect, whereas the chondroprotective effect was not observed at MA concentrations below 20 μM (Figures 1G and 1H). Therefore, we selected the concentration of MA at 40 μM for the following experiment.

Mulberroside A suppresses the inflammatory responses in IL-1β-induced chondrocytes

To determine the anti-inflammatory effect of MA on OA *in vitro*, IL-1β was applied to stimulate the chondrocytes to mimic the *in vitro* cellular environment of OA. As shown in Figures 2A and 2B, IL-1β upregulated the expression of inflammatory proteins (iNOS, COX-2), whereas the enhancement of inflammatory responses induced by IL-1β could be reversed by the administration of 40 μM MA. Besides, this anti-inflammatory effect of MA was verified by the RT-qPCR analysis, as exhibited in Figure 2C, the mRNA expression of iNOS, COX-2, and IL-6 was increased after the IL-1β stimulation, while MA reversed this change. Primer sequences of target genes for RT-qPCR could be found in Table 1.

Mulberroside A inhibits the catabolism in mice osteoarthritis chondrocytes *in vitro* and *in vivo* experiments

The catabolism in chondrocytes which are the only type of cells in cartilage, together with anabolism, plays a key role in the homeostasis of the cartilage ECM. Metabolic imbalance contributes to the degradation of the ECM of cartilage, which leads to the occurrence of OA.[22] *In vitro*, western blot analysis indicated that IL-1β increased the catabolic protein expression of MMP13, ADAMTS4, and ADAMTS5. However, the administration of MA decreased the accumulation of the above proteins (Figures 3A and 3B). RT-qPCR analysis confirmed the above results, as the relative mRNA expression of MMP3, MMP13, and ADAMTS5 was upregulated in IL-1β-induced chondrocytes, whereas this process could be reversed by MA treatment (Figure 3C). In addition, the data of western blot and

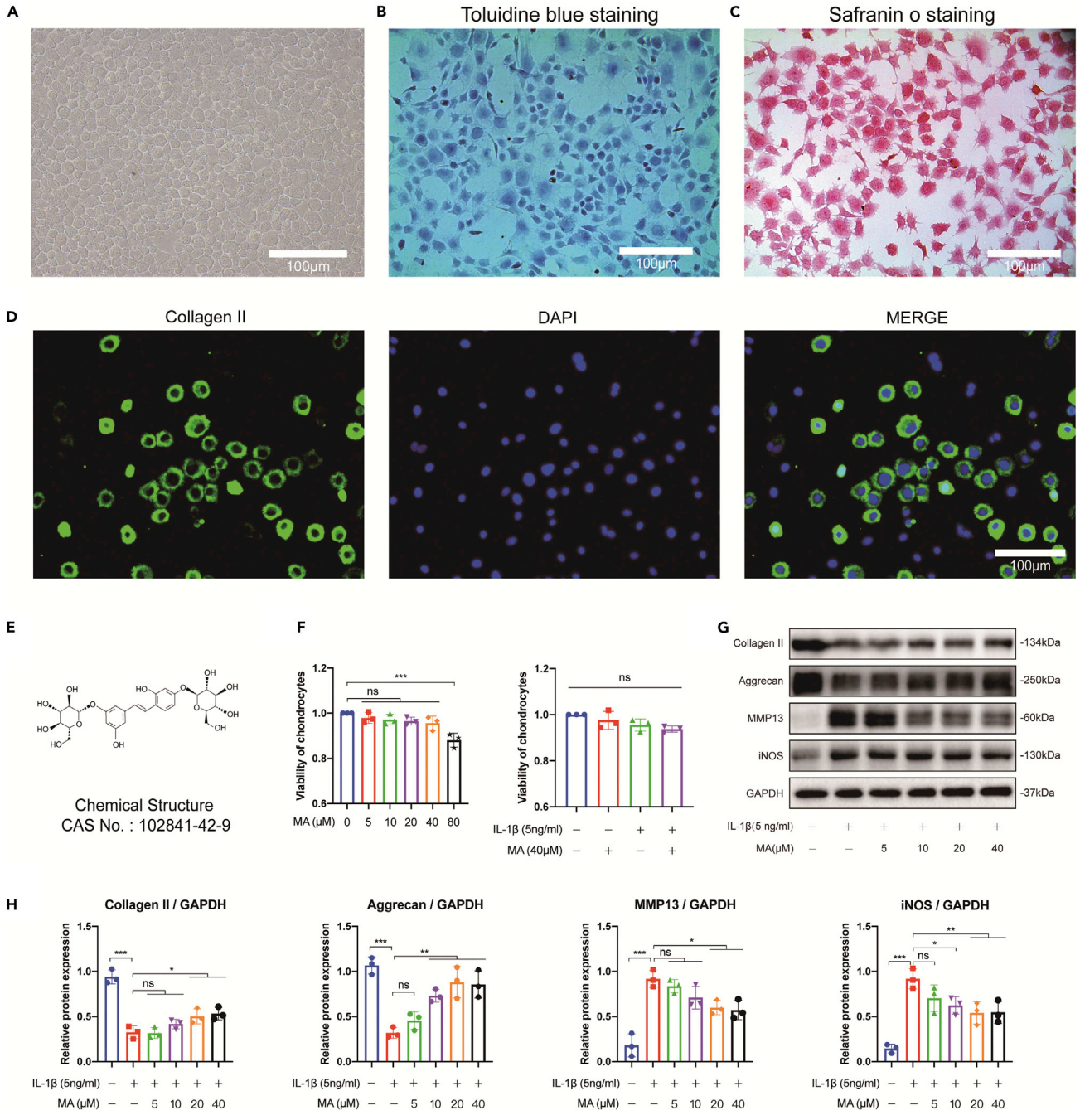

Figure 1. Identification of mice chondrocytes, viability of chondrocytes treated with IL-1β/MA, and selection of an optimal concentration of MA

(A) The general view of primary mice chondrocytes, scalebar = 100 μm.

(B) Toluidine blue staining and (C) Safranin O staining of primary mice chondrocytes, scalebar = 100 μm.

(D) Immunofluorescence staining of Collagen II in primary mice chondrocytes, scalebar = 100 μm.

(E) Chemical structure of MA.

(F) The viability of chondrocytes treated with MA (0, 5, 10, 20, 40, and 80 μM) for 24 h, and with IL-1β (5 ng/mL) or/and MA (40 μM) for 24 h was measured by a CCK-8 kit.

(G) Western blot analysis and (H) quantitative data for anabolic (Aggrecan, Collagen II), catabolic (MMP13), and inflammatory-related (iNOS) proteins in chondrocytes treated with 5 ng/mL IL-1β alone or accompanied with different concentrations of MA (5, 10, 20, and 40 μM). Data were presented as means ± SD (n = 3). ns, no significance; *p < 0.05; **p < 0.01; ***p < 0.001.

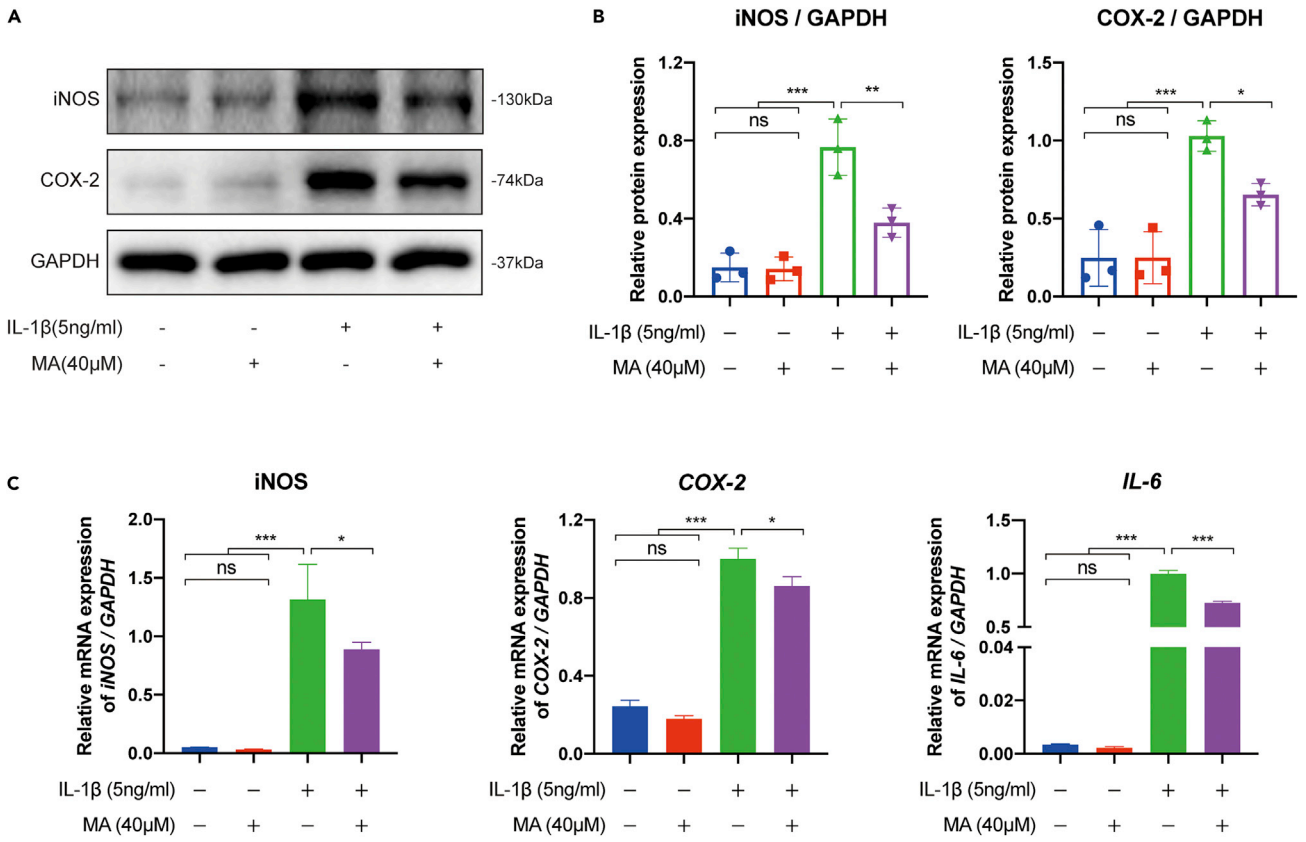

Figure 2. MA suppresses the inflammatory responses in IL-1β-induced chondrocytes

Chondrocytes were treated with IL-1β (5 ng/mL) or/and MA (40 μM) for 24 h.

(A) Western blot analysis and (B) quantitative data for inflammatory proteins (iNOS, COX-2).

(C) The mRNA expression inflammatory genes (iNOS, COX-2, and IL-6) were measured by RT-qPCR analysis. Data were presented as means ± SD (n = 3). ns, no significance; *p < 0.05; **p < 0.01; ***p < 0.001.

RT-qPCR about MMP13 were also verified by immunofluorescence detection, and the high expression of MMP13 induced by IL-1β was inhibited by MA treatment (Figures 3D and 3E). Furthermore, IHC staining (Figures 3F and 3G) revealed that the DMM group developed an increased expression of MMP13 compared with the SHAM and SHAM + MA group, whereas the DMM + MA group reversed the upregulated expression of MMP13 in DMM-induced OA chondrocytes, which was consistent with the results of the *in vitro* experiment.

Mulberroside A promotes the anabolism in mice osteoarthritis chondrocytes *in vitro* and *in vivo* experiments

Studies have shown that the inhibition of chondrocyte anabolism promotes the OA progression.[23] Previous studies have suggested that inflammatory environments can cause anabolism to be blocked, which is consistent with our experimental results, as IL-1β decreased the expression of anabolic proteins including Collagen II, Aggrecan, and SOX9, however, the downregulated trends of anabolic proteins could be reversed by the treatment of MA (Figures 4A and 4B). The above western blot data were verified by RT-qPCR analysis. The inhibited mRNA expression of anabolic-related genes (Aggrecan, Collagen II, SOX9) in IL-1β-induced chondrocytes was reversed by the administration of MA (Figure 4C). Besides, immunofluorescence detection revealed that MA increased the decreased expression of Aggrecan in IL-1β-induced chondrocytes (Figures 4D and 4E). Moreover, IHC staining (Figures 4F and 4G) revealed that the DMM group developed a decreased expression of Aggrecan compared with the SHAM and SHAM + MA group, whereas the DMM + MA group reversed the downregulated expression of Aggrecan in DMM-induced OA cartilage, which was consistent with the results of the *in vitro* experiment.

Table 1. Primer sequence used in the RT-qPCR experiment

Gene	Sequence
Aggrecan	Forward: 5′-CTCACCCCAAGAATCAAGTGG-3′
	Reverse: 5′-GATCTCCAAGGTAGCATCGC-3′
Collagen II	Forward: 5′-CTTAGTGCAGGAAACTTCGCG-3′
	Reverse: 5′-ACCAGGATTGCCTTGAAATCC-3′
S0X9	Forward: 5′-AGCACTCTGGGCAATCTCA-3′
	Reverse: 5′-GTTCACCGATGTCCACGTC-3′
ADAMTS5	Forward: 5′-GCAAAGTGGGCTACCTTGTC-3′
	Reverse: 5′-GTTTCTACAGAGGCACCGTG-3′
MMP3	Forward: 5′-ACTCCCTGGGACTCTACCAC-3′
	Reverse: 5′-GGTACCACGAGGACATCAGG-3′
MMP13	Forward: 5′-GATGGACCTTCTGGTCTTCT-3′
	Reverse: 5′-GCTCATGGGCAGCAACAATA-3′
INOS	Forward: 5′-CTCCTGCCTCATGCCATTG-3′
	Reverse: 5′-AGCTCATCCAGAGTGAGCTG-3′
IL-6	Forward: 5′-TCCAGTTGCCTTCTTGGGAC-3′
	Reverse: 5′-CTGTTGGGAGTGGTATCCTC-3′
COX-2	Forward: 5′-GATAACCGAGTCGTTCTGCC-3′
	Reverse: 5′-AATCCTGGTCGGTTTGATGC-3′
GAPDH	Forward: 5′-TGTTTCCTCGTCCCGTAGAC-3′
	Reverse: 5′-GTTGAGGTCAATGAAGGGGTC-3′

Mulberroside A inhibits the activation of MAPK and NF-κB signaling pathways in IL-1β-induced chondrocytes

MAPK and NF-κB are signaling pathways closely related to the chondrocyte inflammation, which promotes the occurrence of OA.[9] The former includes the JNK, ERK, and P38 signaling pathways, while P65 is the key regulator downstream of the NF-κB signaling pathway. For the two signaling pathways analysis, IL-1β upregulated the protein expression level of the phosphorylation of JNK, ERK, P38, and P65 (*p*-JNK, *p*-ERK, p-P38, and p-P65) compared with the control group, whereas the administration of MA decreased the expression of *p*-JNK, *p*-ERK, p-P38, and p-P65. However, there was no significant change in the protein expression of JNK, ERK, P38, and P65 among the groups. Thus, as illustrated in Figures 5A and 5B, IL-1β triggered the activation of the MAPK and NF-κB signaling pathway, as the ratio of *p*-JNK/JNK, *p*-EC and 5DRK/ERK, p-P38/P38, and p-P65/P65 was increased, whereas MA could suppress the activation process as the above ratio was reversed when MA was administrated in IL-1β-stimulated chondrocytes. In addition, as shown in Figures 5C and 5D, the expression of p-P65 was accumulated in the nuclear after the stimulation of IL-1β, while this nuclear translocation trend of p-P65 could be blocked with the MA treatment.

Mulberroside A inhibits the activation of the PI3K-AKT-mTOR signaling pathway in IL-1β-induced chondrocytes

PI3K-AKT-mTOR signaling pathway, which received much attention due to its role in cartilage degradation, inflammatory responses, and autophagy,[24,25] was investigated in the experiment. As shown in Figures 6A and 6B, IL-1β triggered the significant activation of p-PI3K, *p*-AKT, and *p*-mTOR signaling, as the expression of those proteins increased, while PI3K, AKT, and mTOR maintained a relatively constant expression level among all groups. However, the administration of 40 μM MA decreased the accumulation of proteins p-PI3K, *p*-AKT, and *p*-mTOR, which indicated that MA was provided with the effect of inhibiting the activation of the PI3K-AKT-mTOR signaling pathway.

Mulberroside A attenuates the downregulation of autophagy in IL-1β-induced chondrocytes

Autophagy, an important intracellular clearance mechanism, was considered to be relevant to cellular homeostasis, which was involved in the protection of the articular cartilage from degeneration.[26] In our experiments, the regulation of autophagy was inhibited following the stimulation of IL-1β, whereas MA could

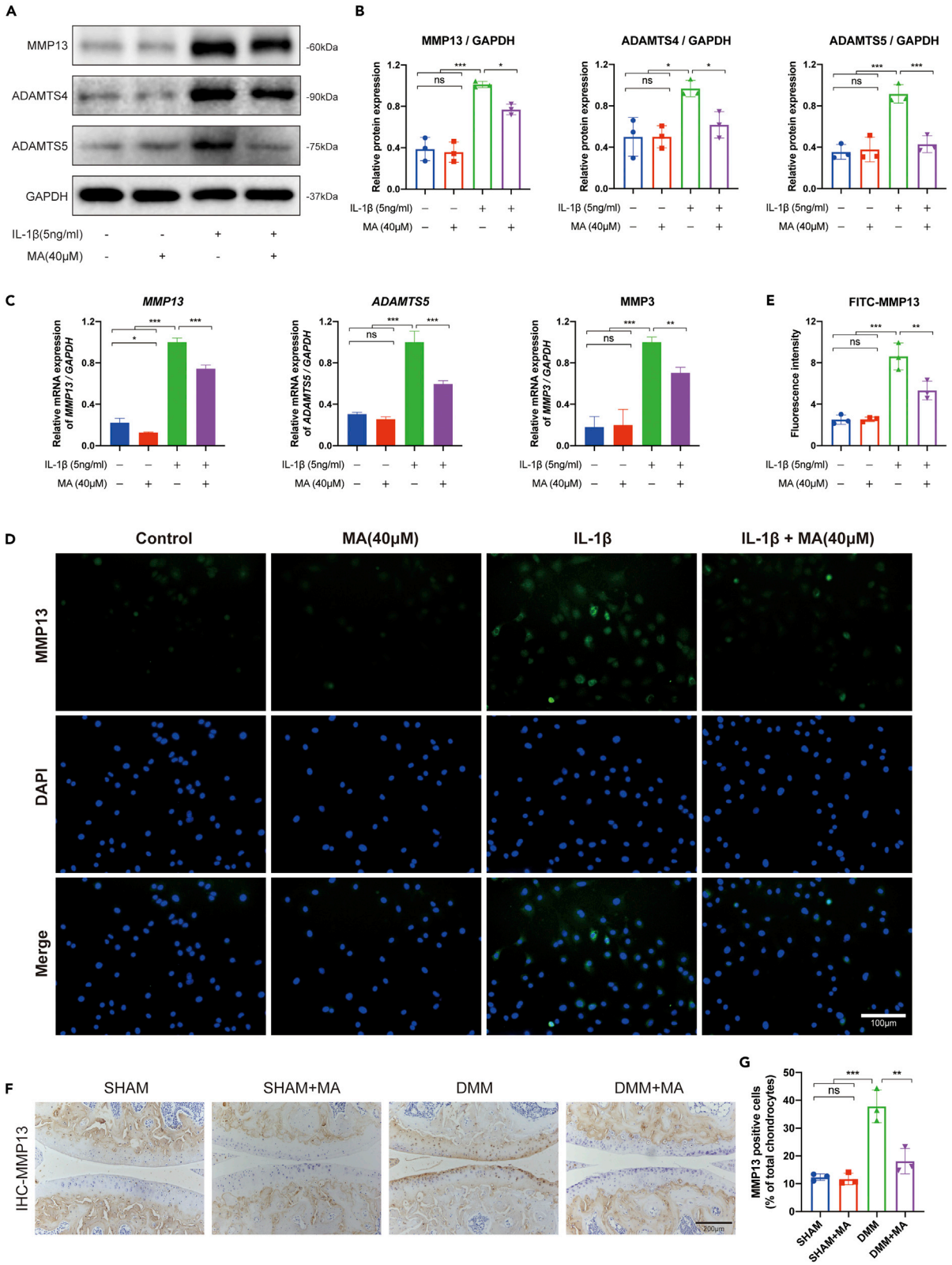
A
MMP13
ADAMTS4
ADAMTS5
GAPDH
-60kDa
-90kDa
-75kDa
-37kDa
IL-1β(5ng/ml)
MA(40μM)
B
MMP13 / GAPDH
ADAMTS4 / GAPDH
ADAMTS5 / GAPDH
Relative protein expression
ns
IL-1β (5ng/ml)
MA (40μM)
C
MMP13
ADAMTS5
MMP3
Relative mRNA expression of MMP13 / GAPDH
Relative mRNA expression of ADAMTS5 / GAPDH
Relative mRNA expression of MMP3 / GAPDH
E
FITC-MMP13
Fluorescence intensity
D
Control
MA(40μM)
IL-1β
IL-1β + MA(40μM)
MMP13
DAPI
Merge
100μm
F
SHAM
SHAM+MA
DMM
DMM+MA
IHC-MMP13
200μm
G
MMP13 positive cells (% of total chondrocytes)

Figure 3. MA inhibits the catabolism in mice OA chondrocytes *in vitro* and *in vivo* experiments

In vitro, chondrocytes were treated with IL-1β (5 ng/mL) or/and MA (40 μM) for 24 h.

(A) Western blot analysis and (B) quantitative data for catabolic-related proteins (MMP13, ADAMTS4, and ADAMTS5) in chondrocytes.

(C) The mRNA expression catabolic-related genes (MMP13, ADAMTS5, and MMP3) were measured by RT-qPCR analysis.

(D) Immunofluorescence staining and (E) quantitative analysis of the expression levels of MMP13, scalebar = 100 μm.

(F) Immunohistological staining and (G) quantitative analysis of catabolic protein MMP13 among groups *in vivo* experiments, scalebar = 200 μm. Data were presented as means ± SD (n = 3). ns, no significance; *p < 0.05; **p < 0.01; ***p < 0.001.

rescue the impaired autophagy. As shown in Figures 6C and 6D, western bolts analysis revealed that IL-1β downregulated the protein expression of the positive regulators of autophagy (Atg3, Atg5, Atg7, Atg12, Beclin-1, and LC3-II/I) and upregulated the negative regulator of autophagy (P62). However, the treatment of MA in IL-1β-induced chondrocytes reversed the above phenomenon, which meant that MA increased the positive regulators and decreased the negative regulator of autophagy. In addition, an autophagy flux detection experiment was performed. The mRFP is used to label and track LC3. The weakening of GFP means that lysosomes and autophagosomes are fused to form autophagolysosomes, then GFP fluorescence is quenched since GFP fluorescent protein is sensitive to acid, and only red fluorescence can be detected at this time, so the strength of autophagic flux can be clearly captured via quantification of different colored spots. As shown in Figures 6E-6G, the data indicated that IL-1β induced the decreased autophagic flux compared with the control group; however, an increased autophagic flux was observed in IL-1β-induced chondrocytes after the administration of MA.

Mulberroside A ameliorates cartilage destruction in mice destabilized medial meniscus osteoarthritis models

Intra-articular injection of MA is to clarify the role of MA in DMM-induced OA models *in vivo* (Figure 7A). From a macroscopic view, as shown in Figure 7B, the DMM group demonstrated OA-related characteristics, including rough articular surface, numerous osteophytes, and narrowed joint space compared with the SHAM and SHAM + MA groups. However, the above OA-like features were seldom seen in the DMM + MA group. Besides, as shown in Figure 7C, analysis of bone remodeling parameters, such as BV, BV/TV, Tb.Sp, Tb.N, and Tb.Th indicated that bone resorption was observed in the DMM group compared with the SHAM and SHAM + MA groups. However, in the DMM + MA group, intra-articular injection with MA relieved the DMM-induced bone resorption, demonstrating that MA has the property of preventing bone loss. From a microscopic view, as shown in Figures 8A-8C, histological staining including H&E, toluidine blue, safranin O/fast green staining revealed significant morphological changes among all groups. As the DMM group exhibited uneven and non-smooth articular surfaces, severe cartilage erosion, and loss of proteoglycan compared with that of the SHAM group and the SHAM + MA group. However, the adverse effects of articular cartilage impairment were ameliorated by MA treatment, as intra-articular injection of MA in DMM-induced OA mice (the DMM + MA group) presented with less cartilage erosion and more proteoglycans compared with that in the DMM group. Besides, the OARSI score, which reflects the degree of articular cartilage destruction, verified that MA ameliorated the progression of OA (Figure 8D).

DISCUSSION

Osteoarthritis (OA), which causes pain, swelling, and limited mobility, is a disease characterized by the degeneration of articular cartilage, synovial hyperplasia, osteophyte formation, subchondral bone sclerosis, and narrowing of the joint space. The treatment of OA is a long-term treatment process. Strategies to manage OA are mainly the conventional medicines used, which have side effects such as liver damage and gastrointestinal discomfort.[27] Therefore, these main symptoms and long-term management of OA can cause great distress and inconvenience to the patient.[28] However, the mechanism of OA is still not fully understood, studies suggest that inflammation and autophagy are closely related to the progression of OA.[29–31]

MA is a natural bioactive ingredient isolated from Mori Cortex. Previous studies have suggested that MA could regulate NF-κB, apoptosis, and EGFR signaling pathway,[11,32] and also play a role in anti-inflammatory,[12] antitussive,[33] anti-hyperuricemia,[14] and anti-melanin formation,[34] anti-kidney cancer.[32] The above-mentioned properties of MA or the signaling pathways regulated by MA may also involve in alleviating OA. Studies suggest that its anti-inflammatory properties are achieved by inhibiting the NF-κB signaling pathway, and its biological properties have not been studied in OA.[16] Previous studies have shown that inflammatory factors can aggravate OA and anti-inflammatory strategies are considered to be beneficial in the treatment of OA.[35] Besides, NF-κB signal pathway is one of the crucial inflammatory signal pathways,

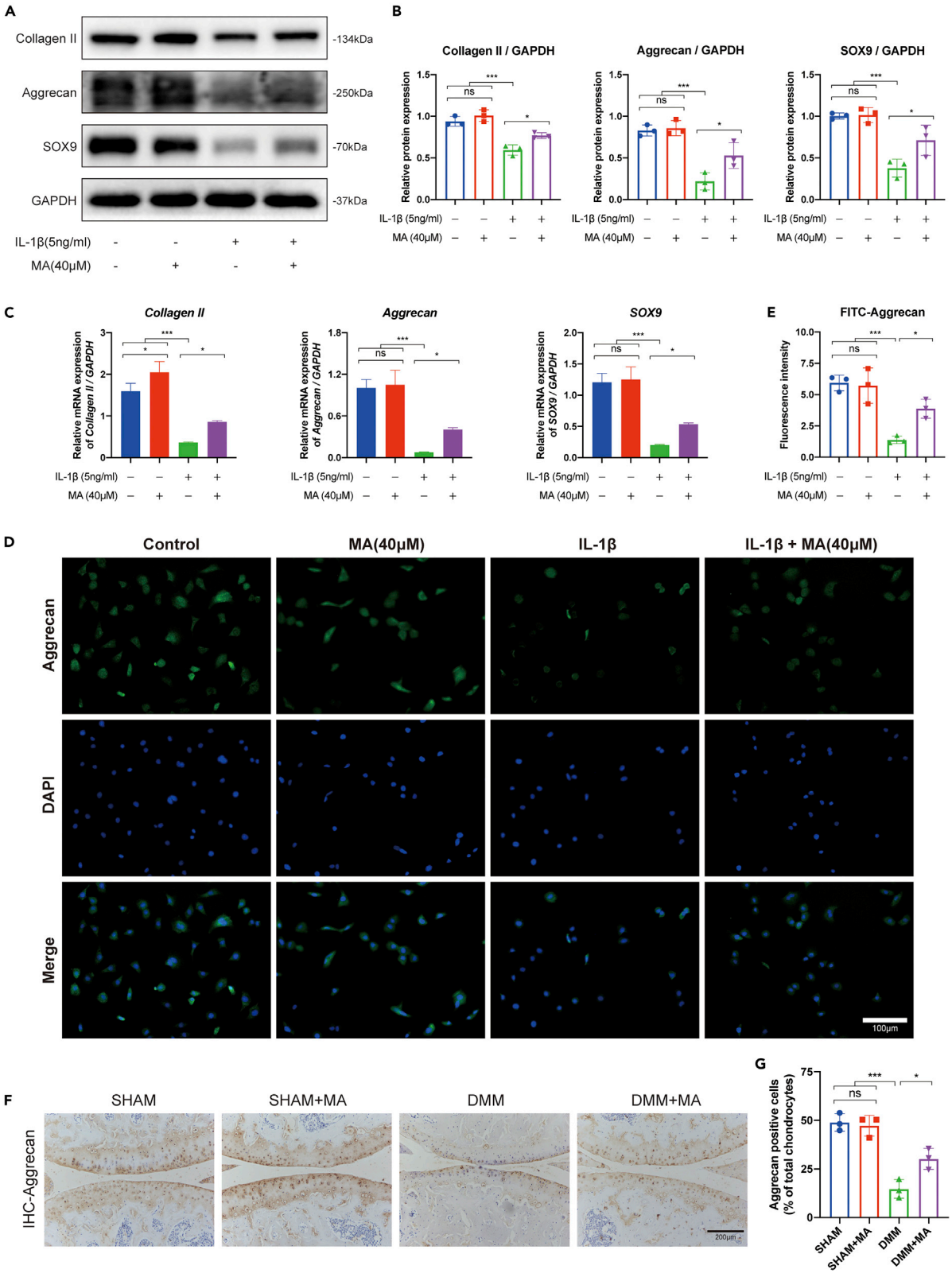
A
Collagen II
Aggrecan
SOX9
GAPDH
-134kDa
-250kDa
-70kDa
-37kDa
IL-1β(5ng/ml)
MA(40μM)
B
Collagen II / GAPDH
Aggrecan / GAPDH
SOX9 / GAPDH
Relative protein expression
IL-1β (5ng/ml)
MA (40μM)
C
Collagen II
Aggrecan
SOX9
Relative mRNA expression of Collagen II / GAPDH
Relative mRNA expression of Aggrecan / GAPDH
Relative mRNA expression of SOX9 / GAPDH
E
FITC-Aggrecan
Fluorescence intensity
D
Control
MA(40μM)
IL-1β
IL-1β + MA(40μM)
Aggrecan
DAPI
Merge
100μm
F
SHAM
SHAM+MA
DMM
DMM+MA
IHC-Aggrecan
200μm
G
Aggrecan positive cells (% of total chondrocytes)

Figure 4. MA promotes the anabolism in mice OA chondrocytes *in vitro* and *in vivo* experiments

In vitro, chondrocytes were treated with IL-1β (5 ng/mL) or/and MA (40 μM) for 24 h.

(A) Western blot analysis and (B) quantitative data for anabolic-related proteins (Aggrecan, Collagen II, and SOX9) in chondrocytes.

(C) The mRNA expression anabolic-related genes (Aggrecan, Collagen II, and SOX9) were measured by RT-qPCR analysis.

(D) Immunofluorescence staining and (E) quantitative analysis of the expression levels of Aggrecan, scalebar = 100 μm.

(F) Immunohistological staining and (G) quantitative analysis of anabolic protein Aggrecan among groups *in vivo* experiments, scalebar = 200 μm. Data were presented as means ± SD (n = 3). ns, no significance; *p < 0.05; **p < 0.01; ***p < 0.001.

the activation of which is involved in the progression of OA, and the inhibition of this signal pathway could alleviate OA progression.[36] In addition, the PI3K-AKT-mTOR pathway is also an important inflammatory signaling pathway which associates with NF-κB signaling pathway, as AKT could trigger the activation of NF-κB signal and contribute to the production of inflammatory mediators.[37,38] Thus, in this study, we explored the role of MA in inflammatory signaling pathways in chondrocytes and revealed that MA was a protective agent against the progression of OA via suppressing the MAPK, NF-κB, and PI3K-AKT-mTOR signaling pathways and promoting the autophagy process in IL-1β-induced chondrocytes.

The phenotypes of anabolic and catabolic in chondrocytes play crucial in maintaining extracellular matrix homeostasis (ECM) in cartilage.[39] As key indicators of anabolism, Aggrecan, Collagen II, and SOX9 are crucial in maintaining the physiological characteristics of cartilage. Collagenase-mediated or aggrecanase-induced degradation of collagen or aggrecan contributed to the loss of Collagen II and Aggrecan in early OA.[40–42] Among the aggrecanases in mouse cartilage, ADAMTS5 and ADAMTS4 are the most important members of the ADAMTS family which could contribute to the cleavage of Aggrecan.[43,44] As for catabolism, MMP13 is the most critical enzymes in chondrocyte catabolism among the many catabolic enzymes, which degrade Collagen II and Aggrecan and lead to the destruction of ECM.[45] In addition, the imbalance of pro-inflammatory and anti-inflammatory responses is an important factor leading to the progression of osteoarthritis. Previous research found that long-term chronic inflammatory response can lead to the weakening of cartilage anabolism and the enhancement of catabolism, which in turn triggers the degradation of the extracellular matrix and the occurrence and development of OA.[46] And controlling the inflammatory response can prevent or slow the progression of the disease. IL-1β, a commonly used inflammatory factor in OA *in vitro* models, can upregulate inflammatory markers (iNOS, COX-2, and IL-6), however, the administration of MA downregulated the inflammatory response. Combined with the cartilage anabolism-promoting and catabolism-inhibiting effects of MA, it indicates that MA possesses the chondroprotective property through anti-inflammatory effects.

The MAPK and NF-κB signaling pathways are crucial factors in the regulation of inflammatory response and are closely related to many diseases, including OA.[47,48] Studies have revealed that the activation of the two signaling pathways could upregulate the expression of inflammatory proteins (iNOS, COX-2, and IL-6) and catabolic proteins (MMP1, MMP3, MMP13, and ADAMTS5), as well as downregulate the expression of anabolic proteins (Aggrecan, Collagen II, and SOX9), which in turn facilitate the degradation of ECM and cartilage destruction.[18,49–51] Measurements of the inhibition of the MAPK and NF-κB signal transduction could prevent or slow the development of OA.[52,53] The PI3K-AKT-mTOR pathway is one of the important inflammatory signaling pathways leading to the progression of OA.[54] Studies have suggested the protein AKT, which regulates the upstream IkB kinases of NF-κB signaling pathway, triggers the activation of NF-κB signal.[37] Inhibiting the PI3K-AKT-mTOR pathway relieves the inflammatory response and is beneficial for the relief of OA.[55] What is more, the PI3K-AKT-mTOR pathway is considered to be a key pathway in the regulation of autophagy.[56,57] The downstream regulator mTOR of the PI3K-AKT-mTOR pathway could manage the autophagy process in a negatively regulated manner, thus inhibiting the PI3K-AKT-mTOR pathway promoting autophagy.[58] Our data revealed that IL-1β successfully established the OA chondrocytes model, as the MAPK, NF-κB, and PI3K-AKT-mTOR signaling pathways are activated under such conditions. However, the administration of MA inhibits the activation of the MAPK, NF-κB, and PI3K-AKT-mTOR pathways, reflecting the protective effect of MA on OA chondrocytes.

Autophagy is a key intracellular clearance mechanism that can remove harmful molecules or damaged organelles, maintain normal cellular life activities, protect the ECM of articular cartilage from degradation and relieve OA development.[59] Autophagy mainly includes three forms, macroautophagy, microautophagy, and chaperone-mediated autophagy.[60] Among them, macroautophagy is the most common and the most widely studied. As a major regulator in the process of autophagy, the expression of positive regulators of autophagy is usually upregulated, while the negative regulator of autophagy downregulated with

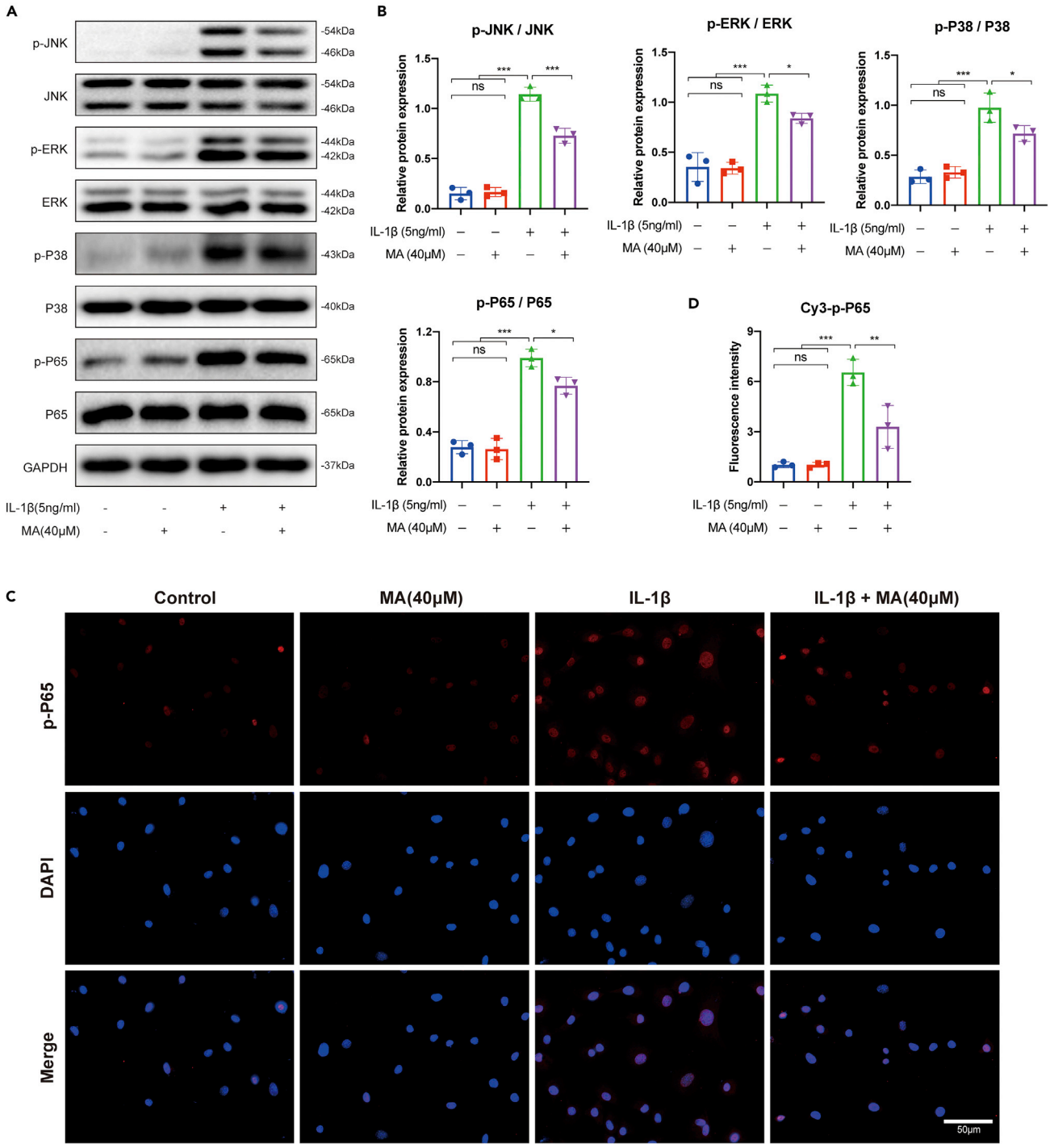

Figure 5. MA inhibits the activation of MAPK and NF-κB signaling pathways in IL-1β-induced chondrocytes

Chondrocytes were pretreated with MA (40 μM) for 24 h, then stimulated with or without IL-1β (5 ng/mL) for 15 min.

(A) Western blot and (B) quantitative analysis showed the activation of MAPK (JNK, ERK, and P38) and NF-κB (P65) signaling pathway induced by IL-1β could be inhibited by the administration of MA (40 μM).

(C) Immunofluorescence staining and (D) quantitative analysis of the nuclear translocation of p-P65 in chondrocytes, scalebar = 50 μm. Data were presented as means ± SD (n = 3). ns, no significance; *p < 0.05; **p < 0.01; ***p < 0.001.

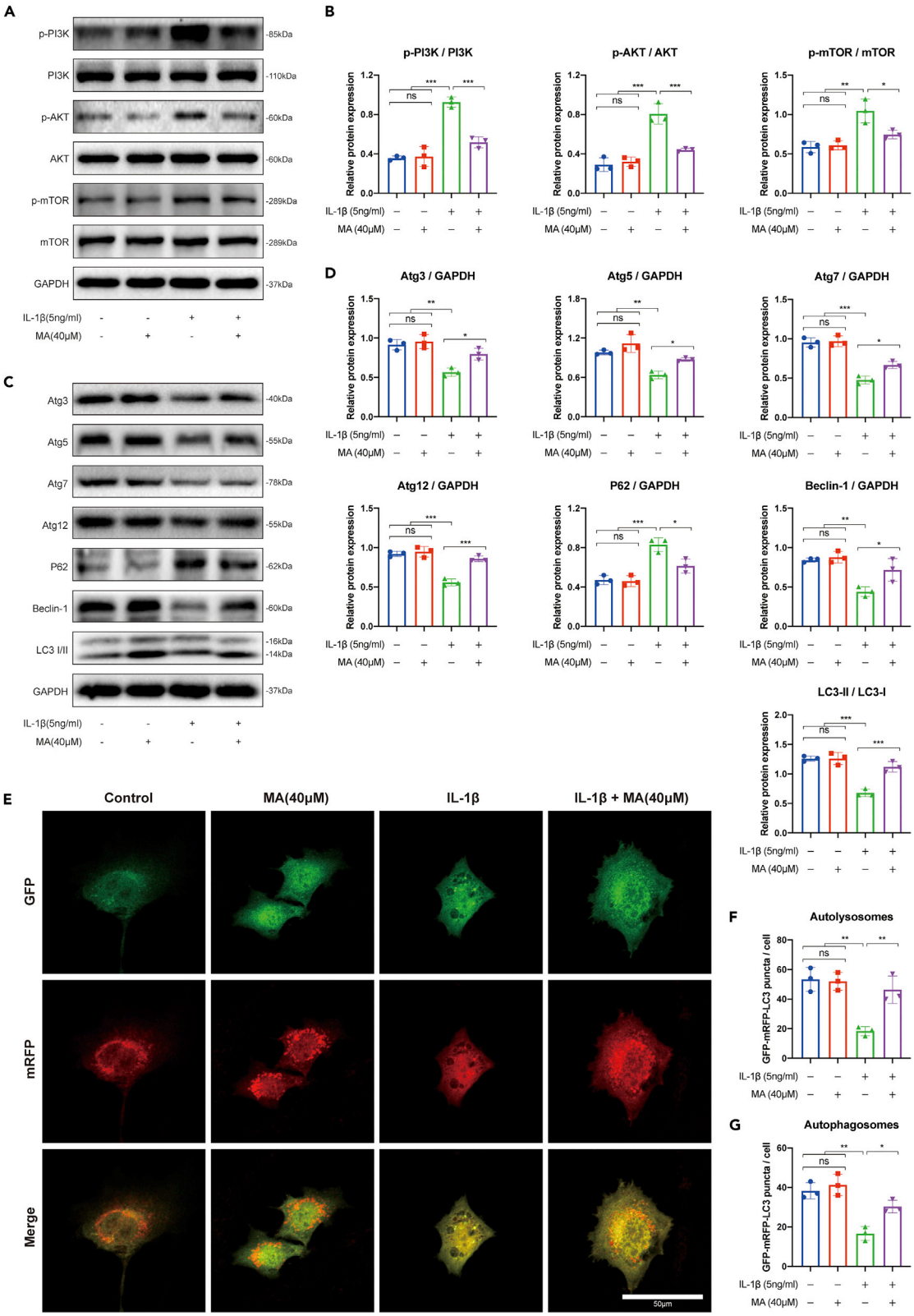
A
p-PI3K
PI3K
p-AKT
AKT
p-mTOR
mTOR
GAPDH
-85kDa
-110kDa
-60kDa
-60kDa
-289kDa
-289kDa
-37kDa
IL-1β(5ng/ml) - - + +
MA(40μM) - + - +
C
Atg3
Atg5
Atg7
Atg12
P62
Beclin-1
LC3 I/II
GAPDH
-40kDa
-55kDa
-78kDa
-55kDa
-62kDa
-60kDa
-16kDa
-14kDa
-37kDa
IL-1β(5ng/ml) - - + +
MA(40μM) - + - +
B
p-PI3K / PI3K
p-AKT / AKT
p-mTOR / mTOR
Relative protein expression
ns
***
**
*
IL-1β (5ng/ml) – – + +
MA (40μM) – + – +
D
Atg3 / GAPDH
Atg5 / GAPDH
Atg7 / GAPDH
Atg12 / GAPDH
P62 / GAPDH
Beclin-1 / GAPDH
LC3-II / LC3-I
E
Control
MA(40μM)
IL-1β
IL-1β + MA(40μM)
GFP
mRFP
Merge
50μm
F
Autolysosomes
GFP-mRFP-LC3 puncta / cell
G
Autophagosomes

Figure 6. MA inhibits the activation of the PI3K-AKT-mTOR signaling pathway and restores the impaired autophagy in IL-1β-induced chondrocytes

Chondrocytes were pretreated with MA (40 μM) for 24 h, then stimulated with or without IL-1β (5 ng/mL) for 1 h.

(A) Western blot and (B) quantitative analysis showed the activation of the PI3K-AKT-mTOR signaling pathway induced by IL-1β could be suppressed by the administration of MA (40 μM). Chondrocytes were treated with IL-1β (5 ng/mL) or/and MA (40 μM) for 24 h.

(C) Western blot and (D) quantitative analysis showed the impaired autophagy induced by IL-1β could be rescued by the administration of MA (40 μM).

(E-G) Chondrocytes transfected with adenovirus labeled with the mRFP and GFP to track LC3 protein, scalebar = 50 μm. Data were presented as means ± SD (n = 3). ns, no significance; *p < 0.05; **p < 0.01; ***p < 0.001.

the enhancement of autophagy activity. The formation of autophagosome is managed by a series of proteins, including the positive regulators (Atg3, Atg5, Atg7, Atg12, Beclin-1, and LC3-II/I) and the negative regulator (P62). Studies have demonstrated that the deletion of autophagy-indispensable Atg5 gene could result in the loss of proteoglycans and occurrence of age-related OA.[61] In addition, the reduced autophagic activity of chondrocytes leads to a decrease in the phagocytic ability of MMP13, leading to the accumulation of MMP13 and aggravating the development of OA.[62] Enhanced autophagy process is beneficial in OA chondrocytes and can alleviate the progression of OA.[25] Our data indicated that the decreased expression of Atg-related proteins, the reduction of LC3-II/LC3-I ratio, and the accumulation of P62 weakened the autophagic activity, causing the dysregulation of anabolism and catabolism in IL-1β-induced OA chondrocytes, whereas the administration of MA could reverse the above trend and enhance the autophagy signaling pathway, which could alleviate OA.

To summarize, as shown in Figure 8E, our *in vitro* data demonstrated that MA reversed the effects of anabolism-inhibiting, catabolism-enhancing, and inflammation-promoting in IL-1β-induced chondrocytes by suppressing the MAPK, NF-κB, and PI3K-AKT-mTOR signaling pathways and promoting the autophagy process. The *in vivo* experiments revealed that the erosion of knee cartilage and the change of anabolic and catabolic-related markers such as Aggrecan and MMP13 induced in the DMM group could be attenuated by the treatment of MA. These findings indicate that MA may be a new potential strategy for OA treatment. However, our study also has some shortcomings.

Limitations of the study

Firstly, in our study, we did not set a positive control to compare the chondroprotective effects of MA with other clinical drugs for OA treatment, such as NSAIDs and chondroitin sulfate. Secondly, the conclusion gained in our manuscript was that MA played a role in improving OA through restoring impaired autophagy and suppressing the MAPK/NF-κB/PI3K-AKT-mTOR signaling pathways, but this may not be the only mechanism by which MA demonstrated protective effects on articular cartilage, as other signaling pathways might also be involved. At the same time, we did not introduce pathway activators or blockers associated with the MAPK, NF-κB, and PI3K-AKT-mTOR signaling pathways, indicating a relatively weak level of evidence. Thirdly, the mechanism by which MA protects articular cartilage has only been confirmed *in vitro* experiments in mice and needs to be verified *in vivo* experiments. In addition, the direct targets or other potential mechanisms of MA on OA remain to be further explored. In view of the promising therapeutic effects of MA on OA in mice revealed by our study, further work is needed.

STAR★METHODS

Detailed methods are provided in the online version of this paper and include the following:

- KEY RESOURCES TABLE
- RESOURCE AVAILABILITY
  - Lead contact
  - Materials availability
  - Data and code availability
- EXPERIMENTAL MODEL AND SUBJECT DETAILS
  - Animals
  - Extraction and culture of mouse chondrocytes
  - DMM–induced mice OA models
- METHOD DETAILS
  - Cell viability
  - Safranin O staining and toluidine blue staining
  - Western blot analysis

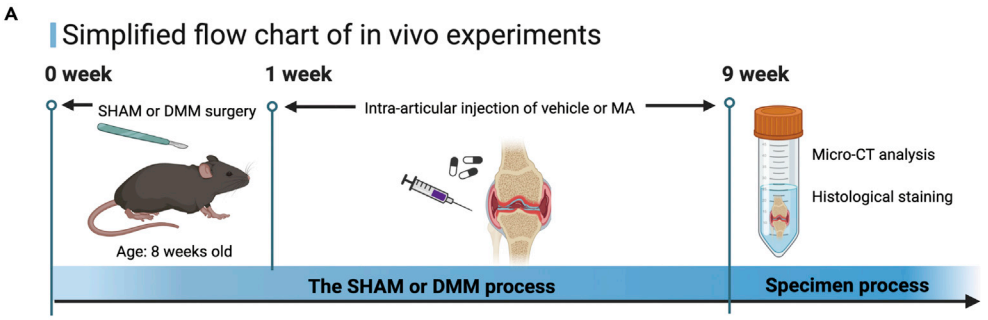
A
Simplified flow chart of in vivo experiments
0 week
1 week
9 week
SHAM or DMM surgery
Intra-articular injection of vehicle or MA
Micro-CT analysis
Histological staining
Age: 8 weeks old
The SHAM or DMM process
Specimen process

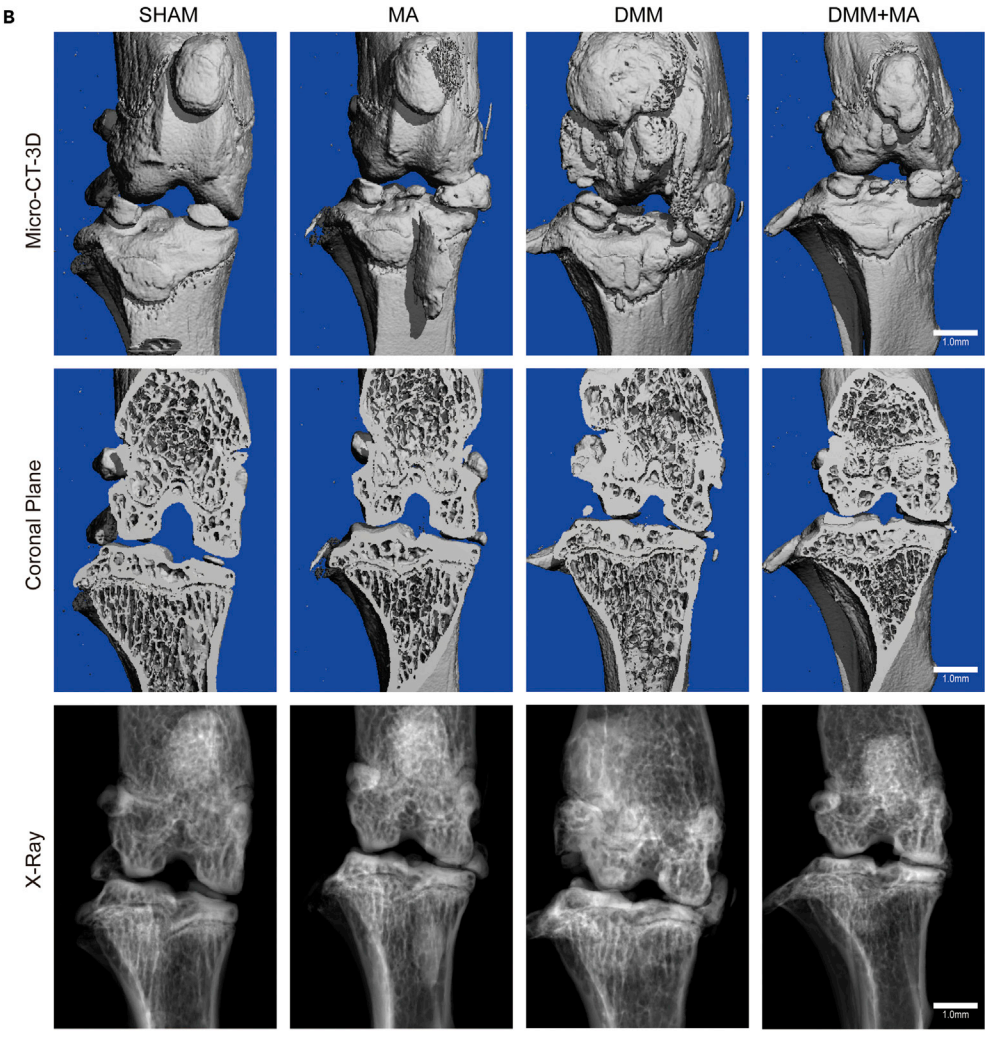
B
SHAM
MA
DMM
DMM+MA
Micro-CT-3D
Coronal Plane
X-Ray
1.0mm

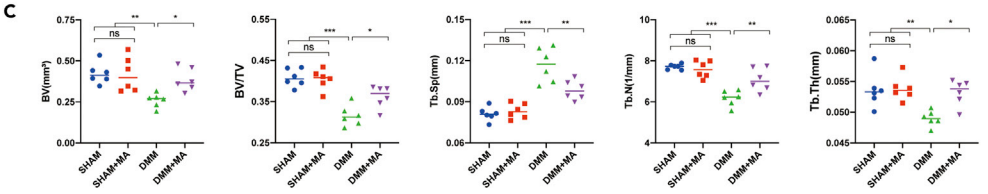
C
BV(mm³)
BV/TV
Tb.Sp(mm)
Tb.N(1/mm)
Tb.Th(mm)
SHAM
SHAM+MA
DMM
DMM+MA

Figure 7. MA alleviates OA-related changes in mice DMM models from a macroscopic view

(A) Simplified flow chart of *in vivo* experiments.

(B) Representative images of micro-CT analysis (Micro-CT-3D, Coronal Plane, and X-ray) reflected the smoothness of cartilage surface, the number of osteophytes formed, and the size of joint space of the knee joints in each group, scalebar = 1.0 mm.

(C) Quantitative analysis of parameters (BV, BV/TV, Tb.Sp, Tb.N, and Tb.Th) that reflected the remodeling of subchondral bone at tibial plateau in knee joints in each group. Data were presented as means ± SD (n = 6). ns, no significance; *p < 0.05; **p < 0.01; ***p < 0.001.

ACKNOWLEDGMENTS

This study was supported by the National Natural Science Foundation of China (No. 81672168, China). We thank Haoran Xu sincerely for his help in this research.

AUTHOR CONTRIBUTIONS

Conceptualization, Rui Lu, Fengjing Guo, Shuang Liang, and An-min Chen; data curation, Rui Lu, Zhenni Wei, Zhenggang Wang, Xiaojian Huang, Hongbo You, Shuang Liang, and An-min Chen; formal analysis, Zhenni Wei, and Zhenggang Wang; funding acquisition, An-min Chen; methodology, Rui Lu, Zhenni Wei, Shimeng Xu, Xiaojian Huang, and Hongbo You; project administration, Fengjing Guo and An-min Chen; software, Kai Sun and Peng Cheng; supervision, Fengjing Guo and Shuang Liang; validation, Shimeng Xu, Kai Sun, Peng Cheng, Xiaojian Huang, and Hongbo You; visualization, Kai Sun and Peng Cheng; writing – original draft, Rui Lu, Zhenni Wei, and Zhenggang Wang; writing – review & editing, Rui Lu, Shuang Liang, and An-min Chen.

DECLARATION OF INTERESTS

The authors declare no competing interests.

INCLUSION AND DIVERSITY

We support inclusive, diverse, and equitable conduct of research.

Received: October 3, 2022
Revised: November 11, 2022
Accepted: January 4, 2023
Published: February 17, 2023

REFERENCES

1. Glyn-Jones, S., Palmer, A.J.R., Agricola, R., Price, A.J., Vincent, T.L., Weinans, H., and Carr, A.J. (2015). Osteoarthritis. Lancet *386*, 376–387. https://doi.org/10.1016/s0140-6736(14)60802-3.

2. Xia, B., Di, C., Zhang, J., Hu, S., Jin, H., and Tong, P. (2014). Osteoarthritis pathogenesis: a review of molecular mechanisms. Calcif. Tissue Int. *95*, 495–505. https://doi.org/10.1007/s00223-014-9917-9.

3. Mandl, L.A. (2019). Osteoarthritis year in review 2018: clinical. Osteoarthritis Cartilage *27*, 359–364. https://doi.org/10.1016/j.joca.2018.11.001.

4. Palazzo, C., Nguyen, C., Lefevre-Colau, M.M., Rannou, F., and Poiraudeau, S. (2016). Risk factors and burden of osteoarthritis. Ann. Phys. Rehabil. Med. *59*, 134–138. https://doi.org/10.1016/j.rehab.2016.01.006.

5. Pritzker, K.P.H., Gay, S., Jimenez, S.A., Ostergaard, K., Pelletier, J.P., Revell, P.A., Salter, D., and van den Berg, W.B. (2006). Osteoarthritis cartilage histopathology: grading and staging. Osteoarthritis Cartilage *14*, 13–29. https://doi.org/10.1016/j.joca.2005.07.014.

6. Mokuda, S., Nakamichi, R., Matsuzaki, T., Ito, Y., Sato, T., Miyata, K., Inui, M., Olmer, M., Sugiyama, E., Lotz, M., and Asahara, H. (2019). Wwp2 maintains cartilage homeostasis through regulation of Adamts5. Nat. Commun. *10*, 2429. https://doi.org/10.1038/s41467-019-10177-1.

7. Mobasheri, A., Rayman, M.P., Gualillo, O., Sellam, J., van der Kraan, P., and Fearon, U. (2017). The role of metabolism in the pathogenesis of osteoarthritis. Nat. Rev. Rheumatol. *13*, 302–311. https://doi.org/10.1038/nrrheum.2017.50.

8. van den Bosch, M.H.J. (2021). Osteoarthritis year in review 2020: biology. Osteoarthritis Cartilage *29*, 143–150. https://doi.org/10.1016/j.joca.2020.10.006.

9. Yang, X., Zhou, Y., Chen, Z., Chen, C., Han, C., Li, X., Tian, H., Cheng, X., Zhang, K., Zhou, T., and Zhao, J. (2021). Curcumenol mitigates chondrocyte inflammation by inhibiting the NF-κB and MAPK pathways, and ameliorates DMM-induced OA in mice. Int. J. Mol. Med.

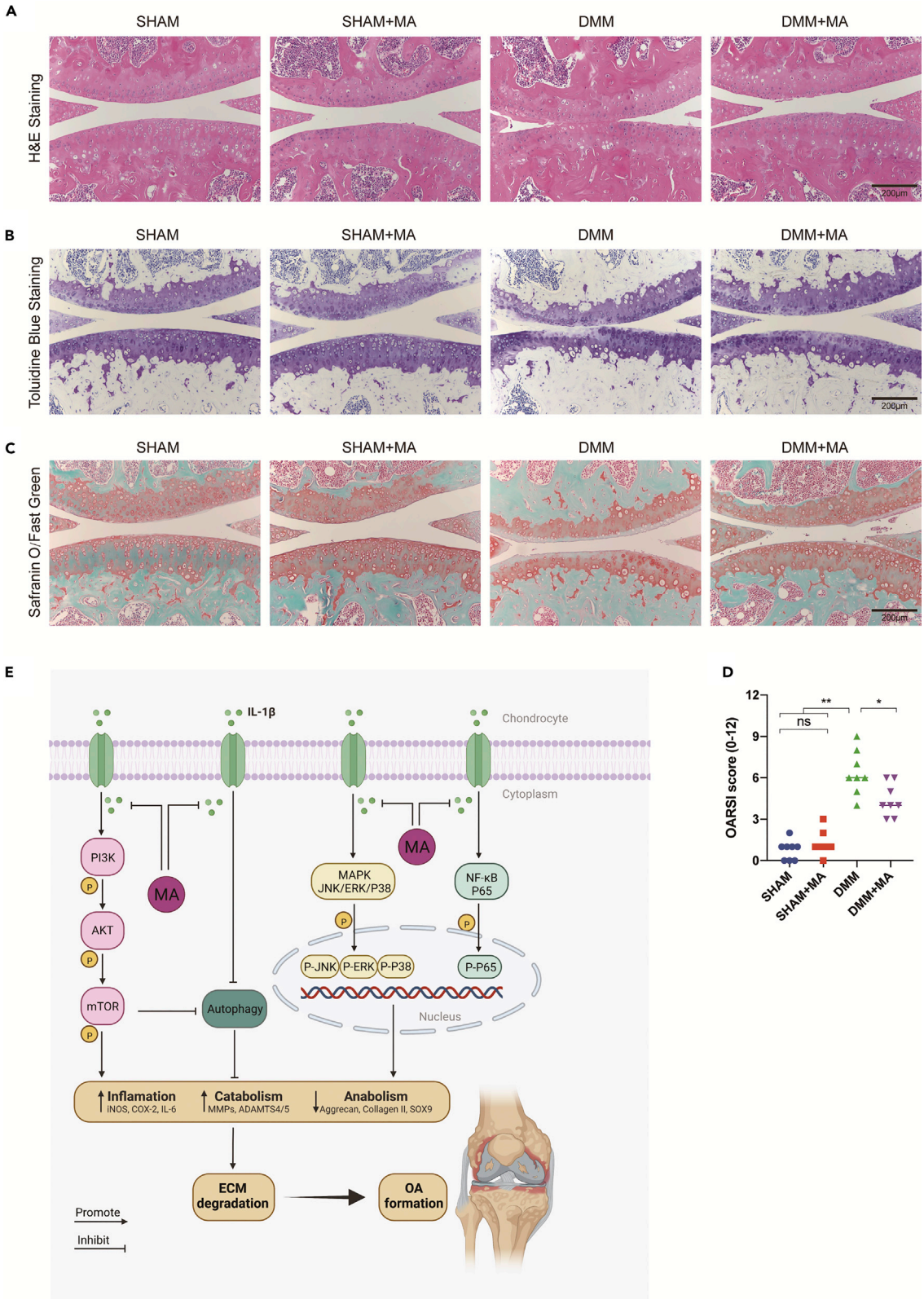
A
SHAM
SHAM+MA
DMM
DMM+MA
H&E Staining
200μm
B
SHAM
SHAM+MA
DMM
DMM+MA
Toluidine Blue Staining
200μm
C
SHAM
SHAM+MA
DMM
DMM+MA
Safranin O/Fast Green
200μm
E
IL-1β
Chondrocyte
Cytoplasm
PI3K
P
AKT
P
mTOR
P
MA
Autophagy
MA
MAPK
JNK/ERK/P38
P
NF-κB
P65
P
P-JNK
P-ERK
P-P38
P-P65
Nucleus
Inflamation
iNOS, COX-2, IL-6
Catabolism
MMPs, ADAMTS4/5
Anabolism
Aggrecan, Collagen II, SOX9
ECM
degradation
OA
formation
Promote
Inhibit
D
OARSI score (0-12)
12
9
6
3
0
ns
**
*
SHAM
SHAM+MA
DMM
DMM+MA

Figure 8. MA ameliorates OA-related changes in mice DMM models from a microscopic view

Histological analysis including.

(A) H&E staining, (B) toluidine blue staining, (C) safranin O/fast green staining of the articular cartilage surfaces, scalebar = 200 μm.

(D) Quantitative analysis of the OARSI scores (n = 8). Data were presented as means ± SD (n = 8). ns, no significance; *p < 0.05; **p < 0.01; ***p < 0.001.

(E) Schematic diagram of the protective effect of MA on mice OA. IL-1β was applied to induce the OA chondrocytes. The effects of inflammation-enhancing, catabolism-promoting, and anabolism-inhibiting induced by IL-1β could be reversed by the treatment of MA. Mechanistically, MA could inhibit the activation of the MAPK, NF-κB, and PI3K-AKT-mTOR signaling pathways in IL-1β induced chondrocytes. In addition, the impaired autophagy process induced by IL-1β could also restored with the administration of MA.

48, 192. https://doi.org/10.3892/ijmm.2021.5025.

10. Valenti, M.T., Dalle Carbonare, L., Zipeto, D., and Mottes, M. (2021). Control of the autophagy pathway in osteoarthritis: key regulators, therapeutic targets and therapeutic strategies. Int. J. Mol. Sci. *22*, 2700. https://doi.org/10.3390/ijms22052700.

11. Chung, K.O., Kim, B.Y., Lee, M.H., Kim, Y.R., Chung, H.Y., Park, J.H., and Moon, J.O. (2003). In-vitro and in-vivo anti-inflammatory effect of oxyresveratrol from Morus alba L. J. Pharm. Pharmacol. *55*, 1695–1700. https://doi.org/10.1211/0022357022313.

12. Zhang, Z., and Shi, L. (2010). Anti-inflammatory and analgesic properties of cis-mulberroside A from Ramulus mori. Fitoterapia *81*, 214–218. https://doi.org/10.1016/j.fitote.2009.09.005.

13. Shi, Y.W., Wang, C.P., Liu, L., Liu, Y.L., Wang, X., Hong, Y., Li, Z., and Kong, L.D. (2012). Antihyperuricemic and nephroprotective effects of resveratrol and its analogues in hyperuricemic mice. Mol. Nutr. Food Res. *56*, 1433–1444. https://doi.org/10.1002/mnfr.201100828.

14. Wang, C.P., Wang, Y., Wang, X., Zhang, X., Ye, J.F., Hu, L.S., and Kong, L.D. (2011). Mulberroside a possesses potent uricosuric and nephroprotective effects in hyperuricemic mice. Planta Med. *77*, 786–794. https://doi.org/10.1055/s-0030-1250599.

15. Park, K.T., Kim, J.K., Hwang, D., Yoo, Y., and Lim, Y.H. (2011). Inhibitory effect of mulberroside A and its derivatives on melanogenesis induced by ultraviolet B irradiation. Food Chem. Toxicol. *49*, 3038–3045. https://doi.org/10.1016/j.fct.2011.09.008.

16. Li, Y., Huang, L., Sun, J., Wei, X., Wen, J., Zhong, G., Huang, M., and Bi, H. (2017). Mulberroside A suppresses PXR-mediated transactivation and gene expression of P-gp in LS174T cells. J. Biochem. Mol. Toxicol. *31*, e21884. https://doi.org/10.1002/jbt.21884.

17. Zhao, C., Liu, Q., and Wang, K. (2017). Artesunate attenuates ACLT-induced osteoarthritis by suppressing osteoclastogenesis and aberrant angiogenesis. Biomed. Pharmacother. *96*, 410–416. https://doi.org/10.1016/j.biopha.2017.10.018.

18. Lu, R., Yu, X., Liang, S., Cheng, P., Wang, Z., He, Z.Y., Lv, Z.T., Wan, J., Mo, H., Zhu, W.T., and Chen, A.M. (2021). Physalin A inhibits MAPK and NF-κB signal transduction through integrin αVβ3 and exerts chondroprotective effect. Front. Pharmacol. *12*, 761922. https://doi.org/10.3389/fphar.2021.761922.

19. Somoza, R.A., and Welter, J.F. (2021). Isolation of chondrocytes from human cartilage and cultures in monolayer and 3D. Methods Mol. Biol. *2245*, 1–12. https://doi.org/10.1007/978-1-0716-1119-7_1.

20. Kim, H.A., and Blanco, F.J. (2007). Cell death and apoptosis in osteoarthritic cartilage. Curr. Drug Targets *8*, 333–345. https://doi.org/10.2174/138945007779940025.

21. Deng, Q., Yu, X., Deng, S., Ye, H., Zhang, Y., Han, W., Li, J., and Yu, Y. (2020). Midkine promotes articular chondrocyte proliferation through the MK-LRP1-nucleolin signaling pathway. Cell. Signal. *65*, 109423. https://doi.org/10.1016/j.cellsig.2019.109423.

22. Malemud, C.J. (2004). Cytokines as therapeutic targets for osteoarthritis. BioDrugs *18*, 23–35. https://doi.org/10.2165/00063030-200418010-00003.

23. Kim, H., Kang, D., Cho, Y., and Kim, J.H. (2015). Epigenetic regulation of chondrocyte catabolism and anabolism in osteoarthritis. Mol. Cell *38*, 677–684. https://doi.org/10.14348/molcells.2015.0200.

24. Huang, C.Y., Lin, H.J., Chen, H.S., Cheng, S.Y., Hsu, H.C., and Tang, C.H. (2013). Thrombin promotes matrix metalloproteinase-13 expression through the PKCδ c-Src/EGFR/PI3K/Akt/AP-1 signaling pathway in human chondrocytes. Mediat. Inflamm.326041 https://doi.org/10.1155/2013/326041.

25. Pan, X., Shan, H., Bai, J., Gao, T., Chen, B., Shen, Z., Zhou, H., Lu, H., Sheng, L., and Zhou, X. (2022). Four-octyl itaconate improves osteoarthritis by enhancing autophagy in chondrocytes via PI3K/AKT/mTOR signalling pathway inhibition. Commun. Biol. *5*, 641. https://doi.org/10.1038/s42003-022-03592-6.

26. Caramés, B., Hasegawa, A., Taniguchi, N., Miyaki, S., Blanco, F.J., and Lotz, M. (2012). Autophagy activation by rapamycin reduces severity of experimental osteoarthritis. Ann. Rheum. Dis. *71*, 575–581. https://doi.org/10.1136/annrheumdis-2011-200557.

27. Marmon, P., Owen, S.F., and Margiotta-Casaluci, L. (2021). Pharmacology-informed prediction of the risk posed to fish by mixtures of non-steroidal anti-inflammatory drugs (NSAIDs) in the environment. Environ. Int. *146*, 106222. https://doi.org/10.1016/j.envint.2020.106222.

28. O'Neill, T.W., and Felson, D.T. (2018). Mechanisms of osteoarthritis (OA) pain. Curr. Osteoporos. Rep. *16*, 611–616. https://doi.org/10.1007/s11914-018-0477-1.

29. Goldring, M.B., and Otero, M. (2011). Inflammation in osteoarthritis. Curr. Opin. Rheumatol. *23*, 471–478. https://doi.org/10.1097/BOR.0b013e328349c2b1.

30. Duan, R., Xie, H., and Liu, Z.Z. (2020). The role of autophagy in osteoarthritis. Front. Cell Dev. Biol. *8*, 608388. https://doi.org/10.3389/fcell.2020.608388.

31. Herrero-Beaumont, G., Pérez-Baos, S., Sánchez-Pernaute, O., Roman-Blas, J.A., Lamuedra, A., and Largo, R. (2019). Targeting chronic innate inflammatory pathways, the main road to prevention of osteoarthritis progression. Biochem. Pharmacol. *165*, 24–32. https://doi.org/10.1016/j.bcp.2019.02.030.

32. Duan, C., Han, J., Zhang, C., Wu, K., and Lin, Y. (2019). Inhibition of kidney cancer cell growth by Mulberroside-A is mediated via mitochondrial mediated apoptosis, inhibition of cell migration and invasion and targeting EGFR signalling pathway. J. BUON *24*, 296–300.

33. Zhaxi, M., Chen, L., Li, X., Komatsu, K., Yao, X., and Qiu, F. (2010). Three major metabolites of mulberroside A in rat intestinal contents and feces. Planta Med. *76*, 362–364. https://doi.org/10.1055/s-0029-1186160.

34. Kim, J.K., Park, K.T., Lee, H.S., Kim, M., and Lim, Y.H. (2012). Evaluation of the inhibition of mushroom tyrosinase and cellular tyrosinase activities of oxyresveratrol: comparison with mulberroside A. J. Enzym. Inhib. Med. Chem. *27*, 495–503. https://doi.org/10.3109/14756366.2011.598866.

35. Wang, C., Gao, Y., Zhang, Z., Chen, C., Chi, Q., Xu, K., and Yang, L. (2020). Ursolic acid protects chondrocytes, exhibits anti-inflammatory properties via regulation of the NF-κB/NLRP3 inflammasome pathway and ameliorates osteoarthritis. Biomed. Pharmacother. *130*, 110568. https://doi.org/10.1016/j.biopha.2020.110568.

36. Lepetsos, P., Papavassiliou, K.A., and Papavassiliou, A.G. (2019). Redox and NF-κB signaling in osteoarthritis. Free Radic. Biol. Med. *132*, 90–100. https://doi.org/10.1016/j.freeradbiomed.2018.09.025.

37. Balwani, S., Chaudhuri, R., Nandi, D., Jaisankar, P., Agrawal, A., and Ghosh, B. (2012). Regulation of NF-κB activation through a novel PI-3K-independent and PKA/Akt-dependent pathway in human umbilical vein endothelial cells. PLoS One *7*, e46528. https://doi.org/10.1371/journal.pone.0046528.

38. Lu, R., He, Z., Zhang, W., Wang, Y., Cheng, P., Lv, Z., Yuan, X., Guo, F., You, H., Chen, A.M., and Hu, W. (2022). Oroxin B alleviates osteoarthritis through anti-inflammation and inhibition of PI3K/AKT/mTOR signaling pathway and enhancement of autophagy. Front. Endocrinol. *13*, 1060721. https://doi.org/10.3389/fendo.2022.1060721.

39. Singh, P., Marcu, K.B., Goldring, M.B., and Otero, M. (2019). Phenotypic instability of chondrocytes in osteoarthritis: on a path to hypertrophy. Ann. N. Y. Acad. Sci. *1442*, 17–34. https://doi.org/10.1111/nyas.13930.

40. Hollander, A.P., Heathfield, T.F., Webber, C., Iwata, Y., Bourne, R., Rorabeck, C., and Poole, A.R. (1994). Increased damage to type II collagen in osteoarthritic articular cartilage detected by a new immunoassay. J. Clin. Invest. *93*, 1722–1732. https://doi.org/10.1172/jci117156.

41. Verma, P., and Dalal, K. (2011). ADAMTS-4 and ADAMTS-5: key enzymes in osteoarthritis. J. Cell. Biochem. *112*, 3507–3514. https://doi.org/10.1002/jcb.23298.

42. Poole, A.R., Kobayashi, M., Yasuda, T., Laverty, S., Mwale, F., Kojima, T., Sakai, T., Wahl, C., El-Maadawy, S., Webb, G., et al. (2002). Type II collagen degradation and its regulation in articular cartilage in osteoarthritis. Ann. Rheum. Dis. *61*. ii78-81. https://doi.org/10.1136/ard.61.suppl_2.ii78.

43. Nagase, H., and Kashiwagi, M. (2003). Aggrecanases and cartilage matrix degradation. Arthritis Res. Ther. *5*, 94–103. https://doi.org/10.1186/ar630.

44. Mead, T.J., and Apte, S.S. (2018). ADAMTS proteins in human disorders. Matrix Biol. *71–72*, 225–239. https://doi.org/10.1016/j.matbio.2018.06.002.

45. Hu, Q., and Ecker, M. (2021). Overview of MMP-13 as a promising target for the treatment of osteoarthritis. Int. J. Mol. Sci. *22*, 1742. https://doi.org/10.3390/ijms22041742.

46. Robinson, W.H., Lepus, C.M., Wang, Q., Raghu, H., Mao, R., Lindstrom, T.M., and Sokolove, J. (2016). Low-grade inflammation as a key mediator of the pathogenesis of osteoarthritis. Nat. Rev. Rheumatol. *12*, 580–592. https://doi.org/10.1038/nrrheum.2016.136.

47. Zhang, Y., Lu, R., Huang, X., Yin, E., Yang, Y., Yi, C., You, H., Song, X., and Yuan, X. (2022). Circular RNA MELK promotes chondrocyte apoptosis and inhibits autophagy in osteoarthritis by regulating MYD88/NF-κB signaling Axis through MicroRNA-497-5p. Contrast Media Mol. Imaging *2022*, 7614497. https://doi.org/10.1155/2022/7614497.

48. Kim, E.K., and Choi, E.J. (2015). Compromised MAPK signaling in human diseases: an update. Arch. Toxicol. *89*, 867–882. https://doi.org/10.1007/s00204-015-1472-2.

49. Sondergaard, B.C., Schultz, N., Madsen, S.H., Bay-Jensen, A.C., Kassem, M., and Karsdal, M.A. (2010). MAPKs are essential upstream signaling pathways in proteolytic cartilage degradation–divergence in pathways leading to aggrecanase and MMP-mediated articular cartilage degradation. Osteoarthritis Cartilage *18*, 279–288. https://doi.org/10.1016/j.joca.2009.11.005.

50. Lu, J., Zhang, H., Pan, J., Hu, Z., Liu, L., Liu, Y., Yu, X., Bai, X., Cai, D., and Zhang, H. (2021). Fargesin ameliorates osteoarthritis via macrophage reprogramming by downregulating MAPK and NF-κB pathways. Arthritis Res. Ther. *23*, 142. https://doi.org/10.1186/s13075-021-02512-z.

51. Choi, M.C., Jo, J., Park, J., Kang, H.K., and Park, Y. (2019). NF-κB signaling pathways in osteoarthritic cartilage destruction. Cells *8*. https://doi.org/10.3390/cells8070734.

52. Deng, Y., Lu, J., Li, W., Wu, A., Zhang, X., Tong, W., Ho, K.K., Qin, L., Song, H., and Mak, K.K. (2018). Reciprocal inhibition of YAP/TAZ and NF-κB regulates osteoarthritic cartilage degradation. Nat. Commun. *9*, 4564. https://doi.org/10.1038/s41467-018-07022-2.

53. You, H., Zhang, R., Wang, L., Pan, Q., Mao, Z., and Huang, X. (2021). Chondro-protective effects of shikimic acid on osteoarthritis via restoring impaired autophagy and suppressing the MAPK/NF-κB signaling pathway. Front. Pharmacol. *12*, 634822. https://doi.org/10.3389/fphar.2021.634822.

54. Tang, Y., Li, Y., Xin, D., Chen, L., Xiong, Z., and Yu, X. (2021). Icariin alleviates osteoarthritis by regulating autophagy of chondrocytes by mediating PI3K/AKT/mTOR signaling. Bioengineered *12*, 2984–2999. https://doi.org/10.1080/21655979.2021.1943602.

55. Xue, J.F., Shi, Z.M., Zou, J., and Li, X.L. (2017). Inhibition of PI3K/AKT/mTOR signaling pathway promotes autophagy of articular chondrocytes and attenuates inflammatory response in rats with osteoarthritis. Biomed. Pharmacother. *89*, 1252–1261. https://doi.org/10.1016/j.biopha.2017.01.130.

56. Tang, Y., Mo, Y., Xin, D., Zeng, L., Yue, Z., and Xu, C. (2020). β-ecdysterone alleviates osteoarthritis by activating autophagy in chondrocytes through regulating PI3K/AKT/mTOR signal pathway. Am. J. Transl. Res. *12*, 7174–7186.

57. Sun, K., Luo, J., Guo, J., Yao, X., Jing, X., and Guo, F. (2020). The PI3K/AKT/mTOR signaling pathway in osteoarthritis: a narrative review. Osteoarthritis Cartilage *28*, 400–409. https://doi.org/10.1016/j.joca.2020.02.027.

58. Al-Bari, M.A.A., and Xu, P. (2020). Molecular regulation of autophagy machinery by mTOR-dependent and -independent pathways. Ann. N. Y. Acad. Sci. *1467*, 3–20. https://doi.org/10.1111/nyas.14305.

59. Arias, C., and Salazar, L.A. (2021). Autophagy and polyphenols in osteoarthritis: a focus on epigenetic regulation. Int. J. Mol. Sci. *23*, 421. https://doi.org/10.3390/ijms23010421.

60. Mahapatra, K.K., Mishra, S.R., Behera, B.P., Patil, S., Gewirtz, D.A., and Bhutia, S.K. (2021). The lysosome as an imperative regulator of autophagy and cell death. Cell. Mol. Life Sci. *78*, 7435–7449. https://doi.org/10.1007/s00018-021-03988-3.

61. Bouderlique, T., Vuppalapati, K.K., Newton, P.T., Li, L., Barenius, B., and Chagin, A.S. (2016). Targeted deletion of Atg5 in chondrocytes promotes age-related osteoarthritis. Ann. Rheum. Dis. *75*, 627–631. https://doi.org/10.1136/annrheumdis-2015-207742.

62. Li, H., Wang, D., Yuan, Y., and Min, J. (2017). New insights on the MMP-13 regulatory network in the pathogenesis of early osteoarthritis. Arthritis Res. Ther. *19*, 248. https://doi.org/10.1186/s13075-017-1454-2.

63. Schmitz, N., Laverty, S., Kraus, V.B., and Aigner, T. (2010). Basic methods in histopathology of joint tissues. Osteoarthritis Cartilage *18*, S113–S116. https://doi.org/10.1016/j.joca.2010.05.026.

64. Yu, T., Guo, F., Yu, Y., Sun, T., Ma, D., Han, J., Qian, Y., Kryczek, I., Sun, D., Nagarsheth, N., et al. (2017). Fusobacterium nucleatum promotes chemoresistance to colorectal cancer by modulating autophagy. Cell *170*, 548–563.e16. https://doi.org/10.1016/j.cell.2017.07.008.

STAR★METHODS

KEY RESOURCES TABLE

REAGENT or RESOURCE	SOURCE	IDENTIFIER
Antibodies		
GAPDH	Proteintech Group, Wuhan, Hubei, China	60004-1-Ig
INOS	Cell Signaling Technology, Beverly, MA, USA	#13120
COX-2	Cell Signaling Technology, Beverly, MA, USA	#12282
MMP13	Proteintech Group, Wuhan, Hubei, China	18165-1-AP
ADAMTS4	Boster, Wuhan, Hubei, China	BA3576-2
ADAMTS5	Boster, Wuhan, Hubei, China	A02802-1
Aggrecan	Proteintech Group, Wuhan, Hubei, China	13880-1-AP
Collagen II	Proteintech Group, Wuhan, Hubei, China	28459-1-AP
SOX9	Cell Signaling Technology, Beverly, MA, USA	#82630
p-JNK	Cell Signaling Technology, Beverly, MA, USA	#4668
JNK	Cell Signaling Technology, Beverly, MA, USA	#9252
p-ERK	Cell Signaling Technology, Beverly, MA, USA	#4370
ERK	Cell Signaling Technology, Beverly, MA, USA	#4695
p-P38	Cell Signaling Technology, Beverly, MA, USA	#4511
P38	Cell Signaling Technology, Beverly, MA, USA	#8690
p-P65	Cell Signaling Technology, Beverly, MA, USA	#3033
P65	Cell Signaling Technology, Beverly, MA, USA	#8242
p-PI3K	Cell Signaling Technology, Beverly, MA, USA	#4228
PI3K	Cell Signaling Technology, Beverly, MA, USA	#4249
p-AKT	Proteintech Group, Wuhan, Hubei, China	66444-1-Ig
AKT	Proteintech Group, Wuhan, Hubei, China	60203-2-Ig
p-mTOR	Proteintech Group, Wuhan, Hubei, China	67778-1-Ig
mTOR	Proteintech Group, Wuhan, Hubei, China	66888-1-Ig
Atg3	Cell Signaling Technology, Beverly, MA, USA	#3415
Atg5	Cell Signaling Technology, Beverly, MA, USA	#12994
Atg7	Cell Signaling Technology, Beverly, MA, USA	#8558
Atg12	Cell Signaling Technology, Beverly, MA, USA	# 4180
Beclin-1	Cell Signaling Technology, Beverly, MA, USA	#3495
P62	Proteintech Group, Wuhan, Hubei, China	18420-1-AP
LC3 I/II	Cell Signaling Technology, Beverly, MA, USA	#12741
HRP Conjugated AffiniPure Goat Anti-mouse IgG	Boster, Wuhan, Hubei, China	BA1050
HRP Conjugated AffiniPure Goat Anti-rabbit IgG	Boster, Wuhan, Hubei, China	BA1054
CY3 Conjugated AffiniPure Goat Anti-rabbit IgG	Boster, Wuhan, Hubei, China	BA1032
FITC Conjugated AffiniPure Goat Anti-rabbit IgG	Boster, Wuhan, Hubei, China	BA1105
Chemicals, peptides, and recombinant proteins		
Mulberroside A	MedChemExpress, Shanghai, China	HY-N0619
Recombinant mouse IL-1β protein	R&D Systems, Minneapolis, MN, USA	NP_032387
Trypsin	Biosharp Life Sciences, Hefei, Anhui, China	BL527A
Collagenase II	Biosharp Life Sciences, Hefei, Anhui, China	BS164
4% Paraformaldehyde	Biosharp Life Sciences, Hefei, Anhui, China	BL539A
DMEM/F12 medium	Hyclone, Logan, UT, USA	SH30023.01

(*Continued on next page*)

Continued

REAGENT or RESOURCE	SOURCE	IDENTIFIER
Fetal bovine serum	BioInd, Biological Industries, Israel	04-001-1ACS
RNA isolation kit	Omega Bio-tek, USA	R6834-01
cDNA synthesis kit	Yeasen, Shanghai, China	11141ES60
RT-qPCR kit	Yeasen, Shanghai, China	11201es08
RIPA lysis buffer	Boster, Wuhan, Hubei, China	AR0102
Protease inhibitors	Boster, Wuhan, Hubei, China	AR1182
Phosphatase inhibitors	Boster, Wuhan, Hubei, China	AR1183
DAPI reagent	Boster, Wuhan, Hubei, China	AR1176
Cell counting kit-8 (CCK-8)	MedChemExpress, Shanghai, China	HY-K0301
Autophagy flow detection kit	HanBio Technology, Shanghai, China	HB-AP2100001
Safranin O Stain Solution	Solarbio Life Sciences, Beijing, China	G1067
Toluidine Blue Stain Solution	Solarbio Life Sciences, Beijing, China	G3660
PVDF membranes	Immobilon, USA	ISEQ00010
SDS-PAGE gels	BioRad, Hercules, CA, USA	4561036
Experimental models: Organisms/strains		
C57BL/6J mouse	GemPharmatech, Nanjing, China	Strain NO.N000013
Primer for RT-qPCR, see Table 1	This paper	N/A
Software and algorithms		
ImageJ Version 1.53 for Mac	National Institutes of Health	https://www.nih.gov/
GraphPad Prism Version 8 for Mac	GraphPad Software	https://www.graphpad.com/
Adobe Illustrator	Adobe	https://www.adobe.com/

RESOURCE AVAILABILITY

Lead contact

Further information and requests for reagents and resources should be directed to and will be fulfilled by the lead contact, Shuang Liang (liangshuang0310@tjh.tjmu.edu.cn).

Materials availability

The study did not generate new unique reagents.

Data and code availability

- All data reported in this paper will be shared by the lead contact upon reasonable request.
- This paper does not report original code.
- Any additional information required to reanalyze the data reported in this paper is available from the lead contact upon request.

EXPERIMENTAL MODEL AND SUBJECT DETAILS

Animals

C57BL/6J mice (Strain NO.N000013) were purchased from GemPharmatech (Nanjing, China). Five days old C57BL/6J male mice were the source of primary chondrocytes *in vitro* and eight weeks old C57BL/6J male mice were employed in our *in vivo* experiment. All experimental procedures were approved by the Institutional Animal Care and Use Committee at Tongji Medical College, Huazhong University of Science and Technology.

Extraction and culture of mouse chondrocytes

Chondrocytes, which were isolated from knee joints of five days old C57BL/6J male mice, were the target cells of our study in *in vitro* experiment. First, mice were sacrificed and disinfected with the help of

immersion in 75% alcohol for 10 min (min). Peel the transparent knee cartilage particles from the joint capsule, remove the synovium, tendon, adipose and other soft tissues around, and cut the cartilage particles into pieces. Then the cartilage particle samples were incubated with 0.25% trypsin for 0.5 h (h) in a cell incubator which containing 5% CO_2. Next, centrifuged and discarded the trypsin, 0.2% collagenase II was added into the chondrocytes for another incubation at 37°C for 4-6 h in a hybridization oven. Then centrifuged and removed the collagenase II, resuspended the chondrocytes, and cultured the chondrocytes in a DMEM/F12 medium containing 10% fetal bovine serum in a cell incubator at 37°C with 5% CO_2. Chondrocytes of the first or second passage were used for experiments.

DMM–induced mice OA models

The destabilized medial meniscus (DMM) surgery was adopted to establish mice OA models in our vivo experiment. Thirty-two C57BL/6J male mice of eight weeks old were randomly and equally divided into two groups (n = 16) and underwent the sham surgery (only underwent joint capsulotomy) and the DMM surgery respectively on the right joint. Then, mice underwent the sham operation were randomly and equally divided into two groups, namely the SHAM group (n = 8) and the SHAM + MA group (n = 8); while mice underwent the DMM operation were randomly and equally divided the DMM group (n = 8) and the DMM + MA group (n = 8). Twice-weekly knee intra-articular injections of vehicle or other treatments for eight consecutive weeks were given one week after surgery. Mice in the SHAM and DMM groups received 10 μL of the vehicle (30% PEG300, 5% DMSO, and ddH2O), while the SHAM + MA group and DMM + MA group received 10 μL of MA (0.091 mg/kg).

METHOD DETAILS

Cell viability

The viability of chondrocytes treated with IL-1β (5 ng/mL) or MA (40 μM) was measured by a cell counting kit-8 (CCK-8). In brief, chondrocytes were cultured in 96-well plates (5,000-10,000 cells/well) for 24 h. Then IL-1β (5 ng/mL) or MA (40 μM) was added into the plates for another 24 h. Next, a CCK-8 reagent was added into the plates and a microplate reader (Bio-Rad, Richmond, USA) was applied to detect the cells' optical density value which reflects the viability of chondrocytes.

Safranin O staining and toluidine blue staining

Chondrocytes are rich in proteoglycans, which can be reflected by safranin o staining.[63] Toluidine blue staining was employed to detect the morphology of chondrocytes with different treatment. The procedure methods of safranin o staining and toluidine blue staining are similarly. Briefly, chondrocytes were pretreated and fixed with 4% paraformaldehyde for 0.25 h. Then removed the fixative reagent and washed the cells with PBS, added the toluidine blue or safranin o reagent into the chondrocytes for staining about 2 h. Next, washed with PBS several times to eliminate the staining reagent and the proteoglycan content or the morphology of chondrocytes could be observed with the help of a microscope.

Western blot analysis

After pretreatment of chondrocytes, the cells were lysed with the lysate reagent which containing RIPA lysis buffer, phosphatase inhibitors, and protease inhibitors. Then collected the cells and lysate mixture into EP tubes for further lysing with an ultrasonic disruptor. Collected the supernatant after centrifugation and measured the concentration of protein samples with a microplate reader. Next, the protein samples were cooked at 100°C for 5 min after thoroughly mixed with the loading buffer. Total protein samples were loaded on the SDS-PAGE with 5% acrylamide in the stacking gel and 8.0–12.5% in the separation gel for electrophoresis. Then proteins were transferred to PVDF membranes. After 1 h of blocking with 5% skim milk, the membranes were incubated with primary antibodies overnight at 4°C and incubated with the corresponding proportion of secondary antibodies for 1 h at 25°C. Finally, a exposure system (Bio-Rad, Hercules, CA, USA) was employed to visualize the target protein bands with the assistant of ECL chemiluminescent substrate (Bio-Rad, Hercules, CA, USA).

RT-qPCR analysis

According to the manufacturer's instructions, a total RNA isolation kit was used to extract RNA from chondrocytes which were undergone different pretreatments. A cDNA synthesis kit was applied to synthesize cDNA from the RNA samples. Then RT-qPCR was performed with the assistant of an RT-qPCR kit

mentioned above. The relative mRNA expression of target genes was measured by calculating the comparative2 $^{-\Delta\Delta Ct}$. Primer sequences of target genes used in the experiment could be found in Table 1.

Immunofluorescence cell staining

Chondrocytes pretreated with IL-1β or with MA were fixed with 4% paraformaldehyde for 0.25 h and then permeabilized with 0.2% Triton X-100 for 5 min. Then the cells were blocked with 5% BSA for 0.5 h and incubated with primary antibodies against Collagen II (28459-1-AP, 1:800, Proteintech, Wuhan, Hubei, China), MMP13 (18165-1-AP, 1:200, Proteintech, Wuhan, Hubei, China), Aggrecan (13880-1-AP, 1:200, Proteintech, Wuhan, Hubei, China), p-P65 (#3033, 1:800, CST, Beverly, MA, USA) overnight at 4°C. Next, removed the primary antibodies and incubated with fluorescent secondary antibody labeled with Cy3 or FITC in the dark for 1 h at 37°C. Then a DAPI reagent (Boster, Wuhan, Hubei, China) was used to stained the nuclei of the chondrocytes. Finally, the pictures were taken by a fluorescence microscope (Evos Fl Auto, Life Technologies, USA).

Autophagy flow detection

After chondrocytes reached about 50% confluence, a autophagy flow detection kit (HanBio Technology, Shanghai, China) was applied in our experiment to detect the autophagy flow[64] which reflects the strength of autophagy under the guidance of the manufacturer. In brief, chondrocytes without pretreatment were transfected with adenoviral labled with mRFP and GFP for 12 h, and cells were cultured continue for 24 h after changing the medium. Then cells were administrated with IL-1β or MA for another 24 h and the autophagy flow was measured with a confocal microscope (Nikon America Inc., Melville, NY). The yellow puncta and the red puncta represented the autophagosomes and autolysosomes respectively.

Micro-computed tomography (micro-CT)

Eight weeks after DMM surgery, the knee joints were obtained and fixed in 4% formaldehyde for 48 h. The high-resolution micro-CT (Scanco Medical, Bassersdorf, Switzerland) was employed to assess the knee samples, and parameters were set as below: X-ray energy at 70 kVP and 112 mA, resolution at 15 mm. Images of micro-CT three-dimensional (micro-CT-3D) and coronal cross-sectional reflected the general view of the knee joints among all groups. Changes in subchondral bone of the mice knee samples were evaluated with indicators such as bone volume (BV), bone volume/tissue volume (BV/TV), trabecular separation (Tb.Sp), trabecular number (Tb.N), and trabecular thickness (Tb.Th).

Histological staining and analysis

After micro-CT analysis, knee joints samples were cut into 5-μm sections after thoroughly decalcified. Histological staining including hematoxylin plus eosin (H&E), toluidine blue, safranin O/fast green, and immunohistochemistry (IHC) was applied in our experiment to determine the severity of articular cartilage damage and the expression of target proteins.

QUANTIFICATION AND STATISTICAL ANALYSIS

All data in the experiment were biologically replicated at least three times and presented as mean ± SD. Student's *t* test was applied to measure the differences between two groups, one-way ANOVA followed by Dunnett's post hoc test was adopted to analyze the data differences among multiple comparisons. Besides, Kruskal-Wallis H test was used to analyzed the nonparametric data (OARSI scores). $p < 0.05$ was considered statistically significant.